Technologies and Processes for the Advancement of Materials

Thermal processing

ISSUE FOCUS ///

BURNERS & COMBUSTION / INSULATING MATERIALS

A NEW LOW-PRESSURE CARBURIZING SOLUTION

COMPANY PROFILE ///

Industrial Physics

FEBRUARY 2023
thermalprocessing.com

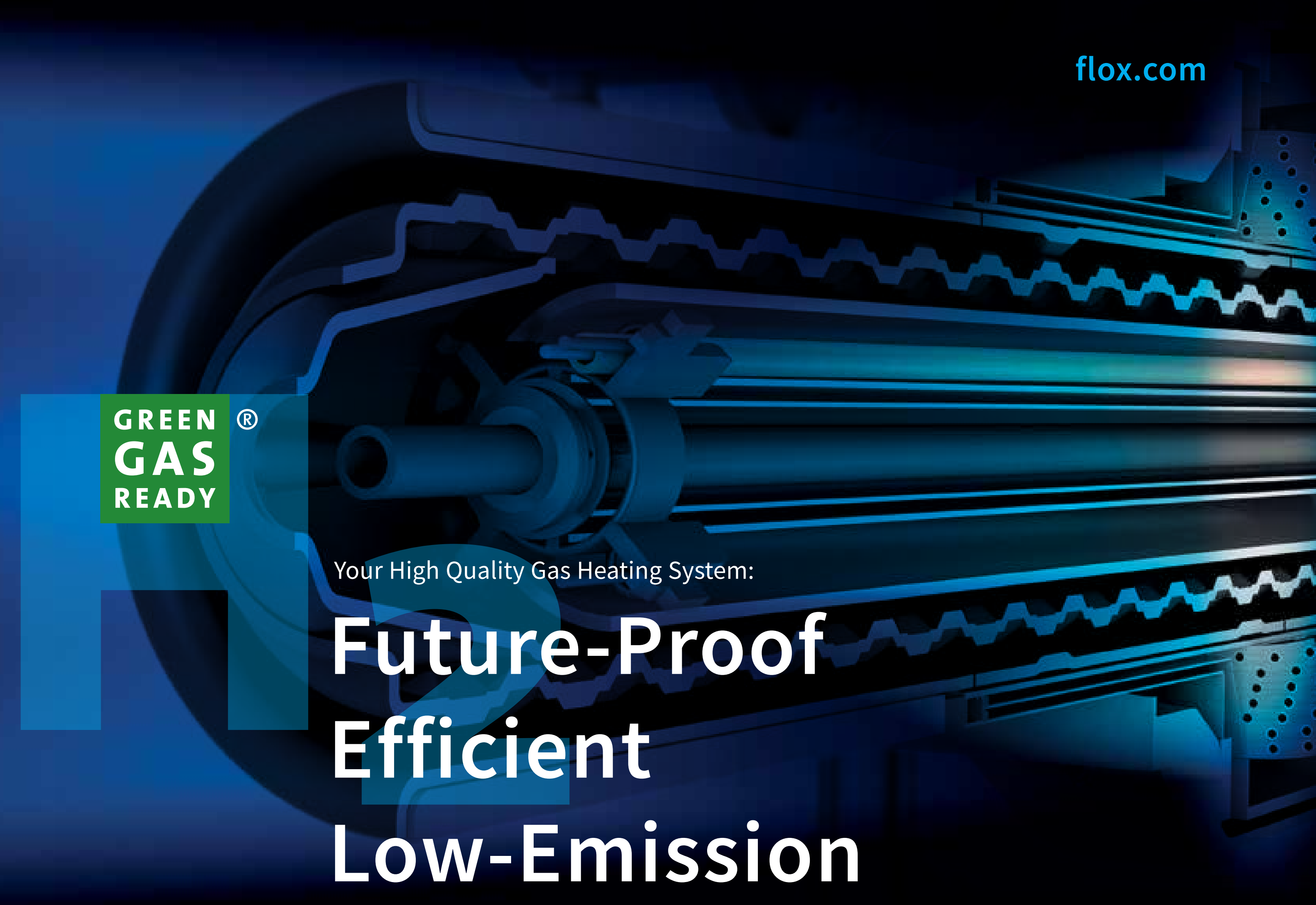

CONTENTS ///

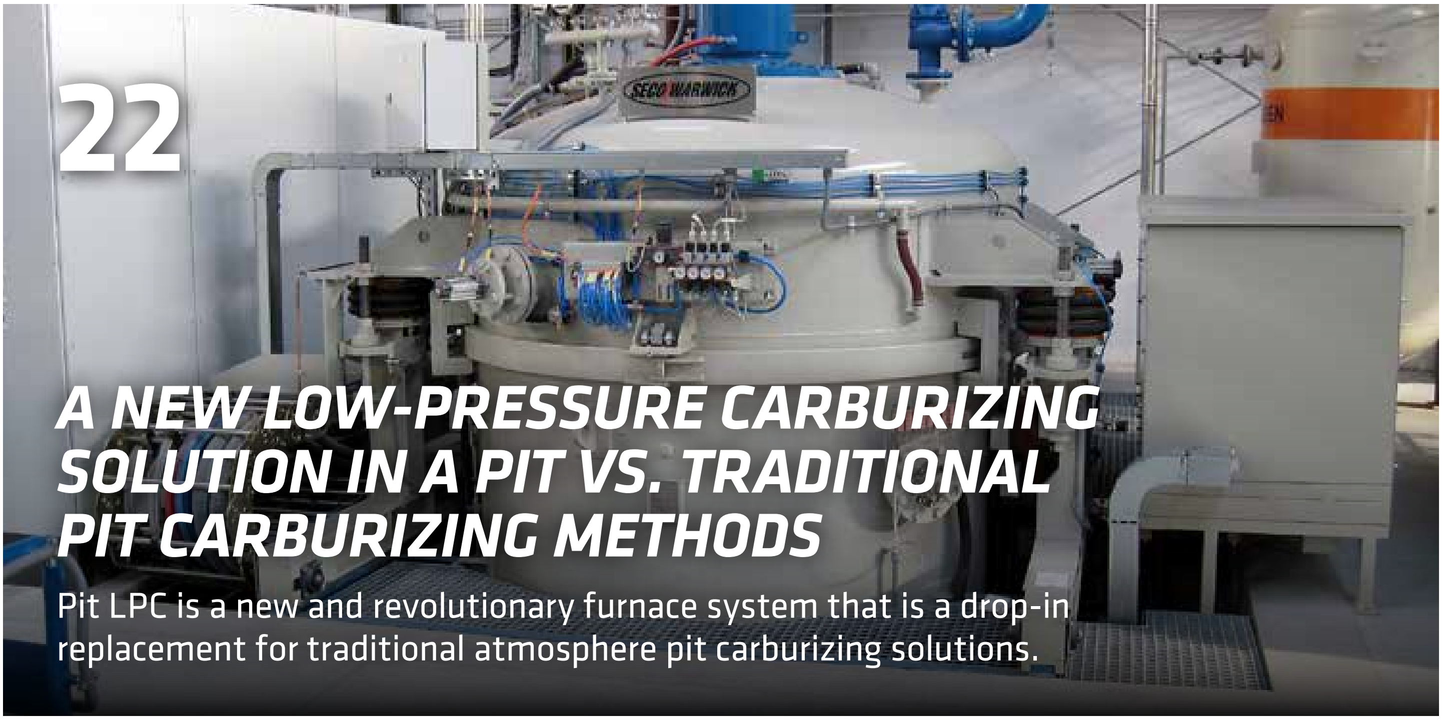

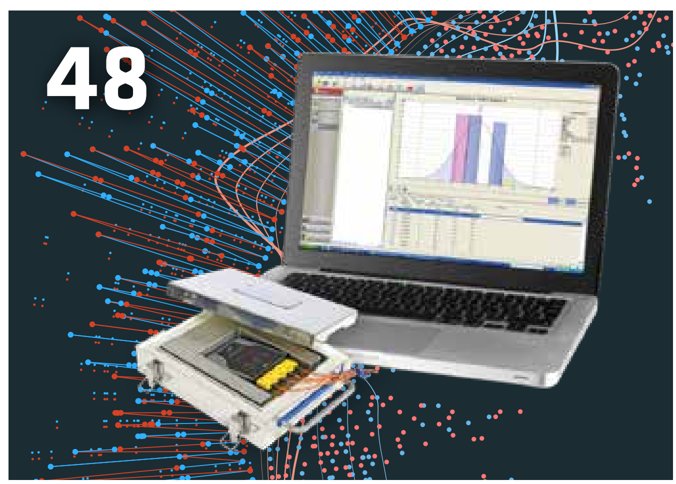

COVER PHOTO: SECO/VACUUM

DEPARTMENTS ///

FEBRUARY 2023 VOLUME 12 / NUMBER 2

Thermal Processing is published monthly by Media Solutions, Inc., 266D Yeager Parkway Pelham, AL 35124. Phone (205) 380-1573 Fax (205) 380-1580 International subscription rates: $105.00 per year. Postage Paid at Pelham AL and at additional mailing offices. Printed in the USA. POSTMASTER: Send address changes to *Thermal Processing* magazine, P.O. Box 1210 Pelham AL 35124. Return undeliverable Canadian addresses to P.O. Box 503 RPO West Beaver Creek Richmond Hill, ON L4B4R6.

Is it February already?

It looks like 2023 is moving at a brisk pace to match the brisk weather.

I hope you feel, as I do, that the world is continuing to move toward a normal pace once again. That should elicit a collective "sigh" from everyone.

To help push that return to a status-quo world, this month's *Thermal Processing* is packed with expert advice as well as insider knowledge and know-how from some of the best the heat-treating world has to offer.

In our Focus section, we take a deep dive with articles discussing burners and combustion as well as a look at new and exciting insulating materials being developed.

Last year, SECO/VACUUM's Tom Hart gave us a little sneak preview in a Q&A of the innovative technology of Pit Low Pressure Carburizing for case hardening large gears. But in our February issue, he takes a deep dive into what makes this new technology a game changer as a revolutionary furnace system that could replace traditional atmosphere pit carburizing solutions. It's a fascinating innovation that is sure to be the talk of the industry in the coming months.

In our second focus article, we take a detailed look into the mechanical properties and thermal conductivity of lightweight and high-strength carbon-graphite thermal insulation materials — an important area of study for aerospace applications.

Another area of interest is an article on plasma and making sure the correct power-delivery systems are in play.

But that's not all. Our columnists are also offering up some solid advice as well.

In Hot Seat, Scott McKenzie talks about quench factor analysis and the C-curve determination.

In Metal Urgency, Jason Meyer looks at the stress modeling of the wire arc additive manufacturing process.

And in Quality Counts, Tony Tenaglier shares his insights on how employers need to expand on the carrot-stick philosophy.

With all that in mind, I hope you enjoy this issue of *Thermal Processing* and find it informative and timely.

And one last thing: Please remember that I'm always looking for fresh, informative articles to share with our readers. Hit me up if you're interested in having your work published.

And, as always, thanks for reading!

KENNETH CARTER, EDITOR
editor@thermalprocessing.com
(800) 366-2185 x204

CALL FOR ARTICLES Have a technical paper or other work with an educational angle? Let Thermal Processing publish it. Contact the editor, Kenneth Carter, at *editor@thermalprocessing.com* for how you can share your expertise with our readers.

Thermal processing

David C. Cooper
PUBLISHER

EDITORIAL

Kenneth Carter
EDITOR

Jennifer Jacobson
ASSOCIATE EDITOR

Joe Crowe
ASSOCIATE EDITOR | SOCIAL MEDIA

SALES

Dave Gomez
NATIONAL SALES MANAGER

Kendall DeVane
REGIONAL SALES MANAGER

CIRCULATION

Teresa Cooper
MANAGER

Jamie Willett
ASSISTANT

DESIGN

Rick Frennea
CREATIVE DIRECTOR

Michele Hall
GRAPHIC DESIGNER

CONTRIBUTING WRITERS

DHAVAL DHAYATKAR
THOMAS HART
JUNCHAO HE
ZHI LIU
YI KANG
D. SCOTT MACKENZIE
JASON MEYER
TONY TENAGLIER
HAIHUA WU
QIANG YANG
XICONG YE
LEI ZHONG
QIANG ZHONG

Media solutions

PUBLISHED BY MEDIA SOLUTIONS, INC.
P. O. BOX 1987 • PELHAM, AL 35124
(800) 366-2185 • (205) 380-1580 FAX

David C. Cooper
PRESIDENT

Teresa Cooper
OPERATIONS

IHEA INDUSTRIAL HEATING EQUIPMENT ASSOCIATION

IFHTSE

Seco/Vacuum, a division of Seco/Warwick Group, will deliver the CaseMaster Evolution to an electric vehicle maker. (Courtesy: Seco/Warwick)

EV manufacturer orders CaseMaster Evolution furnace

A two-chamber CaseMaster Evolution® furnace will be used in an electric vehicle maker's R&D lab to low-pressure carburize (LPC) and oil quench prototype gears.

Currently, the electric vehicle manufacturer sends their prototype gears out to local commercial heat-treatment shops, and there are often scheduling delays. By adding in-house heat treatment capability, the customer is expecting to remove the barriers to accelerating new product development, independent of outside influences.

Seco/Vacuum, a division of Seco/Warwick Group, will deliver the CaseMaster Evolution (CMe) model in the family, with a working hot zone of 16"x16"x24" (400x400x600mm) and a load capacity of 440 lb/200 kg. The CMe-D model has a separate heating chamber, where the product is heated and carburized, and a quenching chamber, where the load is immersed in an oil bath for rapid quenching. Both chambers are isolated with a vacuum door.

The CMe-D 2-chamber vacuum furnace has been proven to be the LPC vacuum carburizing furnace of choice for heat-treating automotive components. It maintains a high-volume throughput of bright, high-quality parts in an economical package. Testing processes with the laboratory configuration allows the customer to move from pilot to large-scale production with predictable performance.

The R&D vacuum furnace order is the latest in a broad range of technologies ordered by this EV manufacturer. Globally, Seco/Warwick Group has cooperated on several other projects, including multiple CAB (controlled atmosphere brazing) equipment for its factory in China for cooling EV batteries, as well as heat treatment and nitriding equipment for tool & die molds in the southwest United States, used to make automotive chassis.

"We have a strong partnership together, having commissioned a number of highly successful heat treat furnaces that provide a wide variety of processes in their plants across the world," said Peter Zawistowski, Seco/Vacuum managing director. "Together with our global parent, Seco/Warwick, we not only provide them with a level of unmatched service, we have an international footprint to support our partner wherever they operate."

Seco/Vacuum is providing a turnkey solution. The scope includes the CMe-D furnace, furnace loader, alloyed fixturing, closed-loop cooling water system and installation.

The oil chamber is equipped with an oil agitation system which provides uniform flow rates throughout the load to reduce distortion. FineCarb®, Seco/Warwick's low-pressure carburizing process, uses acetylene to carburize parts, providing the highest repeatability and uniformity.

The furnace is also equipped with convection heating as well as a gas cooling option, which makes this furnace very flexible, enabling the customer to conduct a wide range of heat-treating procedures to dial in their processes.

MORE INFO www.secowarwick.com

Solar Atmospheres of Michigan plans its future home

Solar Atmospheres of Michigan, formerly Vac-Met, has recently purchased 18,000 square feet of plant space on four-plus acres in Chesterfield, Michigan. The new building is 20 miles northeast of the two existing Vac-Met facilities, which are in Warren and Fraser, Michigan.

"We are working feverishly in 2023 to prepare and equip this new facility to make it our fifth state-of-the-art vacuum heat treating and brazing facility in the United

SEND US YOUR NEWS Companies wishing to submit materials for inclusion in Thermal Processing's Update section should contact the editor, Kenneth Carter, at editor@thermalprocessing.com. Releases accompanied by color images will be given first consideration.

Solar Atmospheres of Michigan has purchased 18,000 square feet of plant space on four-plus acres in Chesterfield, Michigan, for a new facility. (Courtesy: Solar Atmospheres)

States," said Bob Hill, president of Solar Atmospheres of Michigan Inc. "Once all of the electrical, water cooling, and specialty gas utilities are installed, we will strategically relocate the nine existing vacuum furnaces to their new home. Additionally, two new vacuum furnaces were purchased from Solar Manufacturing.

"This investment of over $5 million dollars gives Solar Atmospheres of Michigan the space to locate our valuable employees and equipment under one roof while continuing to grow the Michigan vacuum thermal processing needs."

MORE INFO www.solaratm.com

Heat Treat Mexico 2023 open for registration

Registration is open for Heat Treat Mexico 2023, set for March 28-30 in Monterrey, Mexico. The conference and expo, powered by the strength of the ASM Heat Treating Society, ASM Mexico Chapter, and the organizers of Heat Treat North America, will showcase heat treating resources, programming, and technology for the emerging markets in Mexico.

Attendees can expand their knowledge and stay relevant by attending sessions and workshops that can be applied to day-to-day operations, interact with experts from one of more than 50 exhibitors, and develop relationships with the emerging heat-treating community in Mexico through dedicated networking opportunities.

Along with a new location, the conference offers new session and workshop topics specifically related to the industry in the region, including:

» Aluminum heat treating, principles, and technology.

» Brazing.

» Conventional heat treatment and other manufacturing processes.

» Energy and environment – trends in heat treatment

» Induction heat treatment.

» Metallurgy for the non-metallurgist (full day course).

Registered conference attendees will have access to the following:

» Two and a half days of technical program and workshops.

» Time dedicated to interaction with exhibitors.

» Courses/programs offered in English and Spanish.

» Free one year membership to ASM/HTS for non-members located in Mexico.

» Welcome reception with the exhibitors.

» An evening of professional and social interaction includes live music, open bar and a variety of local food.

» Lunch every day and snacks and drinks during breaks.

MORE INFO www.asminternational.org

Optris IR Sensing LLC makes general management change

Beginning 2023, Optris IR Sensing LLC marked a new chapter in the evolution of the business in the United States as Paul Czerepuszko became president and general manager, replacing Thomas J. Scanlon. Scanlon will continue in the role of senior advisor, leveraging his many years of infrared expertise and management experience.

Scanlon has had a long career in the infrared industry. After 33 years as a successful and experienced sales manager and vice president at FLIR Systems, he established the U.S.-based Optris IR Sensing in partnership with Optris GMBH in 2017. In just over five years, Scanlon developed many successful distribution channels establishing Optris as a major supplier of infrared sensors and IR cameras in the U.S. and Canada.

Paul Czerepuszko

Tom Scanlon

Czerepuszko's focus for the company is to work with the existing team to continue market share expansion and Optris brand recognition in the U.S. and Canada. He is a strong believer in the culture of customer and channel partner support and will make this a priority as he further grows the Optris team in the Portsmouth, New Hampshire, office.

His background qualifies him for his new role as president and general. For most of his 25-year tenure at FLIR Systems, Czerepuszko was fully immersed in developing the automation markets for FLIR's line of infrared cameras.

"Paul can be credited in large part for beginning the adoption of IR cameras for process control and automation applications in the U.S. and his success formula combined application expertise and belief in strong partnerships with distributors and integrators," Scanlon said.

MORE INFO www.optris.com

Registration open for Ceramics Expo set for May

Registration is open for Ceramics Expo, set for May 2-3, 2023, in Novi, Michigan. It will be co-located with Thermal Management Expo North America.

Conference events will cover a variety of technical ceramic applications including aviation, automotive, energy, medical, and electronics. Attendees will be able to:

»Connect and collaborate as they find new suppliers and partners.

»Discover solutions to reduce costs and decrease time to market.

»Find and compare products on the exhibition floor.

»Discuss new products or services directly with the people who can help.

»Meet face to face with engineers, decision makers, end-user OEMs, and buyers from across the globe.

»Learn from high-profile individuals.

»Locate new customers and leads.

The conference program has been designed to address challenges through a series of panels and technical presentations, ensuring attendees can continue to develop in their own role. Popular topics in 2022 included:

»Solving logistics of converting to lower energy-intensive processing techniques for more sustainable operations.

»Understanding the impact of workforce availability on business development and finding out about best solutions to implement positive growth.

»Understanding the impact of business growth on material and manufacturing development capabilities.

»Examining the development of the ceramic market in the coming years and situating the business in the most advantageous position to support and be supported by this growth.

Thermal Management Expo will return for its second year as the only large-scale exhibition and conference dedicated to thermal technologies. Visitors will be able to network with decision-makers and senior engineers from across high-tech industries to source the latest innovations in thermal management technologies, materials, and components.

MORE INFO www.ceramicsexpousa.

L&L Special Furnace Co., Inc. announces new ownership

L&L Special Furnace Co., Inc. has changed ownership. Beginning January 1, 2023, the assets of L&L Special Furnace Co, Inc. were acquired by Specialized Thermal Solutions, Inc.

Gregory Lewicki, left, and David Cunningham. (Courtesy: L&L Special Furnace Co., Inc.)

The company will maintain operations under the name L&L Special Furnace with David Cunningham serving as both owner and president.

Since its beginnings in 1946 as a kiln manufacturer by a pottery entrepreneur and her husband, L&L has undergone many changes, including its relocation in 1979 to a new and larger facility that allowed it to focus on high-end, specialty industrial furnaces. Throughout its history, L&L has remained a family-oriented business dedicated to the needs of its customers.

Gregory Lewicki, son of L&L's founders, began at the company after completing his bachelor's degree from Hobart College in 1973. With his brother, Stephen, he purchased L&L Special Furnace Co., Inc. from their father and moved to a new plant in Aston in 1979. The company grew under the leadership of the two brothers, and in the mid-1990s the pair bought their father's pottery kiln company as well. In 2012, Gregory purchased Stephen's share of L&L Special Furnace Co., Inc., Stephen acquired Gregory's share of L&L Kiln Mfg., Inc., and the two companies became totally separate entities.

Cunningham has been with L&L Special Furnace Co., Inc. since December 2005. In his initial role, he focused on furnace design and purchasing while attending Drexel University in the evenings. He graduated from Drexel in 2009 with a B.S. in applied mechanical engineering, to go along with his A.A.S. in architecture/civil engineering from Pennsylvania Institute of Technology (2003), and A.A.S. in robotics/automated manufacturing from Delaware County Community College (2009). In 2010, he assumed the majority of the furnace design role, handling mechanical design, electrical schematics, controller programming, and some field service. In 2021, Cunningham was appointed general manager of L&L Special Furnace Co., Inc.

Aside from the name change, L&L Special Furnace will remain the same. All contact info and email addresses will remain the same. Specialized Thermal Solutions, Inc. will be absorbing all of L&L Special Furnace Co., Inc.'s order history and will continue to service any of its products.

MORE INFO www.llfurnace.com

AFC-Holcroft hosts open house for employees, families

AFC-Holcroft recently invited employees and their families, company retirees, and other guests to view its newly renovated building as part of an open house.

The purpose of the open house was twofold: to show off the renovations to family and friends and to raise the profile of manufacturing and engineering to school-aged and college- bound students, giving them a real-world look at an actual working environment with a diversity of career options.

Families participated in the factory tour at AFC-Holcroft's newly renovated facility. (Courtesy: AFC-Holcroft)

The day began with general presentation of "what is heat treating" to introduce guests to the "why" of what the company makes. Company president and CEO Bill Disler led each session with a short overview of AFC- Holcroft, highlighting its 100-year history, customer base, global reach, and other aspects.

Following a short 'why and how' of heat treating using common objects to illustrate some of the metallurgical goals of heat treatment, the sessions disbursed among multiple employee volunteers who were stationed around the facility. On the manufacturing floor, guests were given a demonstration of HMI programs, an overview of shipping and receiving areas, and a look at the amount of inventory and spare parts the company carries. They then toured the engineering areas before taking a general tour of the building, where various new environmentally-friendly upgrades and innovative design features have recently been implemented.

At the conclusion of the AFC-Holcroft agenda, guests traveled to nearby Atmosphere Heat Treating, where they got to see fully-operational heat-treating furnaces in operation in an actual commercial heat treatment setting.

"The best work environments are usually those who acknowledge that workers have a life outside of their job, which at times crosses into family time," Disler said. "So, the more the family understands about the work life, the more supportive they may be when those times occur. And on another topic, we also understand the challenges this company and others will face in finding and training the next generation of the workforce. So even in this small way, every opportunity we can find to introduce children to math, science, technology and manufacturing is a win for everyone."

MORE INFO www.afc-holcroft.com

Mark your calendars for these important conference dates

The 5th International Conference on Heat Treatment and Surface Engineering of Tools and Dies will be held in Hangzhou, China, in April.

5TH INTERNATIONAL CONFERENCE ON HEAT TREATMENT AND SURFACE ENGINEERING OF TOOLS AND DIES (HTSE-TD)

Hangzhou, China I April 24-27, 2023

This conference, sponsored by the Chinese Heat Treating Association, will be April 24-27, 2023, in Hangzhou, China. This conference will finally resume the HTSE-TD series. At the present time, it is being planned as in-person conference. The due date deadline for abstracts was January 31, 2023.

ECHT23

Genova, Italy I May 29-31, 2023

AIM is happy to announce the ECHT 2023 Conference in Genova, Italy, at Magazzini del Cotone, May 29-31, 2023.

ECHT 2023 will cover all relevant topics for the Heat Treatment & Surface Engineering community. The Conference will have a special focus on sustainability.

More information: www.aimnet.it/echt2023.htm

Important dates:

- **Abstract Submission Deadline:** December 16, 2022.
- **Notification of acceptance:** January 31, 2023.
- **Preliminary program:** February 27, 2023.
- **Full Paper Submission Deadline:** March 31, 2023.

HEAT TREAT 2023

Detroit, Michigan I October 17-19, 2023

This event will co-located with IMAT 2023 in Detroit, and cover many topics of interest. Abstracts are due February 17, 2023. If an abstract is accepted into the Heat Treat 2023 technical program, the author will be encouraged to submit a full manuscript (6-8 pages) by the deadline date. Complimentary full conference registration will be offered to authors (presenting author only) who submit a full manuscript for the proceedings.

Important dates:

- **Abstracts Due:** February 17, 2023.
- **Accept/Reject Notification:** April 17, 2023.
- **First Draft Manuscript Due:** May 31, 2023.
- **Final PDF Manuscript Due:** July 17, 2023.

28TH IFHTSE CONGRESS

Yokohama, Japan I November 13-16, 2023

This event, sponsored by the Japanese Society for Heat Treatment, will be November 13-16, in Yokohama, Japan. This wide ranging conference will allow participants to network and hear papers on a wide ranging series of topics, including thermal processing of steel, surface hardening additive manufacturing, and modeling and simulation of industrial processes.

Important dates

- **Deadline of abstract submission:** April 28, 2023.
- **Notification of acceptance:** May 31, 2023.
- **Preliminary program release:** June 30, 2023.
- **Deadline of extended abstract:** July 14, 2023.
- **Deadline of early registration:** July 31, 2023.
- **Deadline of full paper submission:** September 22, 2023.

A special issue of JSHT will be published in March 2024 (scheduled). Applicants can submit a full paper (refereed) to the special issue. Only the presenters of the 28th IFHTSE Congress can submit full papers for this special issue.

SPOTLIGHT ON MEMBERS

MISAD

MISAD (Metal Isı İşlem Sanayicileri Derneği) or the Heat Treatment Industrialists Association was established February 25, 2008. Its goal is to provide a common ground for heat-treatment industrialists to meet across Turkey and to establish working standards across Turkey. It is further tasked with organizing and providing technical training for management on quality, management, and heat treatment. Lastly, the organization promotes Turkish heat treaters.

Contact information is misad@misad.org.tr, Kavacık Mah. Fatih Sultan Mehmet Cad. Tonoğlu No:3 İç Kapı No: 4, Beykoz / İstanbul. +90 535 050 4454.

UPCOMING IFHTSE EVENTS

APRIL 24–27, 2023
5th International Conference on Heat Treatment and Surface Engineering of Tools and Dies
Liangzhu Dream Town, Hangzhou, China

MAY 29–31, 2023
ECHT23
Genova, Italy I www.aimnet.it/echt2023.htm

OCTOBER 17–19, 2023
Heat Treat 2023
Detroit, Michigan I www.asminternational.org/web/heat-treat

NOVEMBER 13-16, 2023
28th IFHTSE Congress
Yokohama, Japan

For details on IFHTSE events, go to www.ifhtse.org/events

IFHTSE LEADERSHIP

EXECUTIVE COMMITTEE

Prof. Masahiro Okumiya I President
Toyota Technological Institute I Japan

Eva Troell I Past President
RISE IVF Research Institutes of Sweden I Sweden

Prof. Massimo Pellizzari I Vice President
Dept. of Industrial Engineering, University of Trento I Italy

Dr. Stefan Hock I Secretary General
IFHTSE I Italy

Dr. Imre Felde I Treasurer
Óbuda University I Hungary

OTHER MEMBERS

Prof. Rafael Colas I Universidad Autónoma de Nueva Leon I Mexico
Prof. Jianfeng Gu I Shanghai Jiao Tong University I China
Dr. Patrick Jacquot I Bodycote Belgium, France, Italy I France
Prof. Larisa Petrova I MADI University I Russia
Prof. Reinhold Schneider I Univ. of Appl. Sciences Upper Austria I Austria
Prof. Marcel Somers I Technical University of Denmark I Denmark
Prof. Kewei Xu I Xi'an University I China

ONLINE www.ifhtse.org I **EMAIL** info@ifhtse.org

INDUSTRIAL HEATING EQUIPMENT ASSOCIATION

IHEA rings in 2023 with some great events

IHEA's 2023 Annual Meeting is scheduled for March 13-15 at the One Ocean Resort & Spa in Atlantic Beach, Florida.

FEBRUARY

IHEA's Fundamentals of Industrial Process Heating Online Course starts February 20: IHEA's Fundamentals of Industrial Process Heating Online Learning Course has been a successful source of high-level learning for those in the industrial heat-processing industry for more than 10 years. Registration is now open for the next course, which begins February 20 and runs for six weeks through April 2. The flexible online format and interactive forums are just some of the benefits of this class.

The curriculum includes the basics of heat transfer, fuels and combustion, energy use, furnace design, refractories, automatic control, and atmospheres as applied to industrial process heating. Weekly coursework, quizzes, and a final exam project are administered to guide students on their progress and evaluate their knowledge of the material. For a complete listing of the topics and registration information, go to www.ihea.org/event/FundamentalsFeb23.

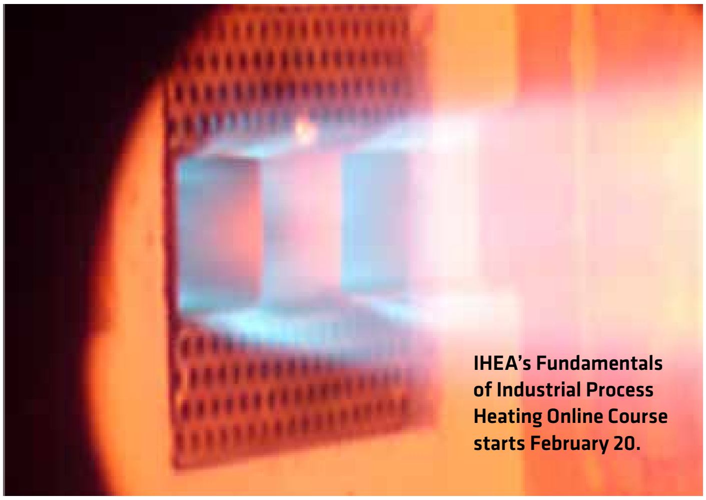

IHEA's Fundamentals of Industrial Process Heating Online Course starts February 20.

IHEA will present a one-day seminar that will focus on the recent changes to NFPA 86 Standard for Ovens and Furnaces. The seminar will be May 23 at the Donald E. Stephens Convention Center in Rosemont, Illinois in conjunction with the Process Heating and Cooling Show.

MARCH

Join IHEA Members at the 2023 Annual Meeting: Scheduled for March 13-15 at the One Ocean Resort & Spa in Atlantic Beach, Florida, the 2023 IHEA Annual Meeting program is set, and registration is open. IHEA has a terrific slate of speakers on the agenda that will bring value to all attendees. There will also be the traditional social events for members and guests to meet and mingle, which include the welcome reception, golf outing, a luau dinner, and the president's reception and gala to close out the event.

Registration is open now. Go to www.ihea.org/event/AM23. IHEA members can use vouchers to register.

MAY

IHEA Offers a One-Day Safety Seminar in conjunction with the Process Heating and Cooling Show: IHEA will present a one-day seminar that will focus on the recent changes to NFPA 86 Standard for Ovens and Furnaces. The seminar will be May 23 at the Donald E. Stephens Convention Center in Rosemont, Illinois in conjunction with the Process Heating and Cooling Show that follows on May 24-25. Seminar attendees will also receive complimentary full conference registration to the exhibition.

This class is the perfect overview for those already familiar with NFPA 86 but want to understand the recent updates and the impact on their business. IHEA instructors are industry experts and NFPA committee members that are directly involved in the development of the standard and revision process.

Registration fee includes a printed copy of the slides and the new 2023 NFPA 86 Standard for Ovens and Furnaces. Watch for details and registration to open soon.

IHEA CALENDAR OF EVENTS

FEBRUARY 30–APRIL 2

Fundamentals of Industrial Process Heating Online Course

This six-week course is designed to give the student a fundamental understanding of the mechanisms of heat transfer within an industrial furnace and the associated losses and the operation of a heating source either as fuel combustion or electricity.

MARCH 13–15, 2023

IHEA 2023 Annual Meeting

One Ocean Resort & Spa I Atlantic Beach, Florida

The Industrial Heating Equipment Association's Annual Meeting is your way to keep current with industry developments and network with peers in the industry.

MARCH 21–22, 2023

Powder Coating & Curing Processes Seminar

Alabama Power Technology Applications Center I Calera, Alabama

The day-and-a-half Introduction to Powder Coating & Curing Processes Seminar will include classroom instruction and hands-on lab demonstrations.

Registration fee: IHEA Members: $325 / Non-Members: $425

For details on IHEA events, go to www.ihea.org/events

JASON MEYER
MECHANICAL ENGINEER /// DANTE SOLUTIONS

Using welding simulation tools to model the direct energy deposition process.

Stress modeling of the WAAM process

A thermal model was previously developed and executed to simulate the Wire Arc Additive Manufacturing (WAAM) process, using the Goldak Flux Distribution to model the welding heat source [1]. The present work focuses on the next step of the modeling process, the stress model.

The natural progression of heat-treatment modeling typically involves executing a thermal model first to predict the temperature changes during the process. Temperature history data are then used to drive the stress model to view results such as in-process and residual stress, phase evolution, distortion, and final hardness and microstructure. The results from the stress model can highlight areas of concern, such as geometric features, which can cause high levels of stress during the process (stress risers), or phase transformation timings, which can cause significant distortion. The results of a stress model can then be used to modify the original geometry, or green shape, to reduce distortion and eliminate stress risers. Process modifications can also be made to reduce the effect of high temperature gradients that will cause distortion in the part.

The stress and thermal models developed were simulated in Abaqus Standard, coupling the QustomWeld [2] and DANTE subroutines. QustomWeld was used to handle modeling the deposition and heating parameters. DANTE was used for the materials and phase transformation models.

STUDY

Some modifications to the previous thermal model were made before execution of the stress model to reduce the gross overheating shown in the first model and to improve model convergence.

A reduction of current during the process was used to reduce the overheating shown in the first analysis.

The mesh along the bead deposition was refined to better capture the thermal gradients present in the process.

The new mesh consists of 27,243 nodes and 21,920 elements (15,123 nodes and 12,000 elements previously).

The convective heat transfer coefficient was slightly increased for the entire process. Coupled with the reduction in current, each pass returns to room temperature during the five-minute cooling between passes.

The build plate material was AISI 1020, and the deposition layers were AISI 1006 low carbon steel.

Otherwise, all other parameters and geometry remain the same.

Low carbon steel is preferred for welding due to its low hardenability, and thus does not typically transform to hard, but brittle, martensite when air cooled. There is a large volume expansion when a steel transforms from austenite to martensite which can also cause high levels of tension in the heat-affected zone. From the analysis results, this filler metal transforms mainly to ferrite and pearlite.

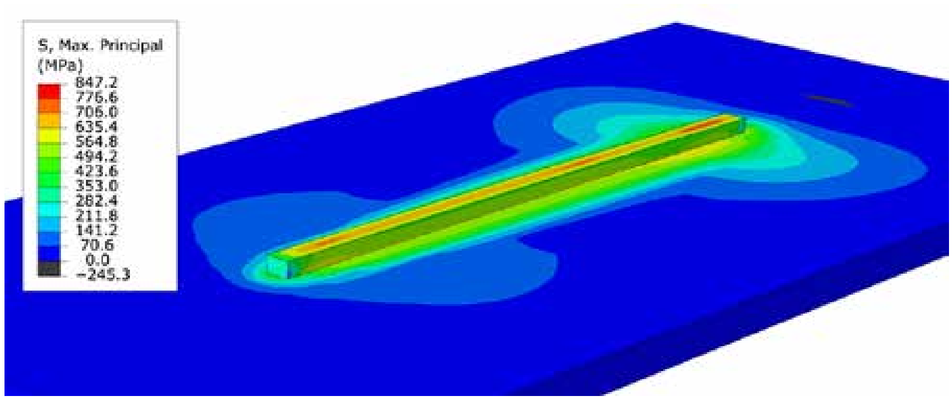

Figure 1: Max principal stress after the first deposition pass and cooled to room temperature.

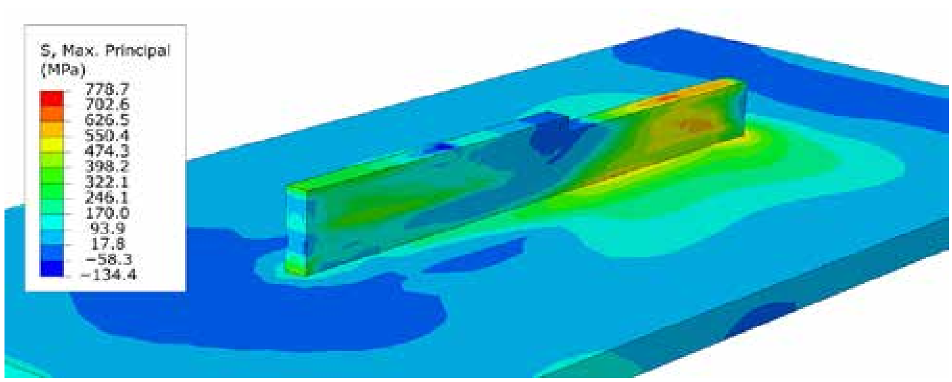

Figure 2: Max principal stress during the fifth deposition pass and cooled to room temperature.

The thermal gradients are extremely steep during the entire process due to the continuous molten pool of material being deposited. These gradients force the stress model to take short time increments to fully characterize the heat transfer during the process. Thus, each of the eight deposition passes required approximately 6,000 increments to solve. Calculation times differ from machine to machine, but this model was executed with eight cores on a workstation PC. The wall clock time for the analysis was just over three days, although a significant portion of that was writing results to the mechanical drive, while about a tenth of that was spent on the actual calculation. This illustrates the challenges of modeling any additive manufacturing process. To effectively model a full 3D printed part, a multi-node server or supercomputer would be required. Regardless, the software, technology, and modeling methods are available once the hardware technology has a chance to catch up.

RESULTS

The results of the stress model show the dynamic changes in stress from pass to pass. Maximum principal stress is used to show the relatively high magnitude of stress during the process and is also used to show what regions are in tri-axial compression. Any region that has compressive maximum principal stress must be in compression in the X, Y, and Z directions. Figure 1 shows the maximum principal stress after the first deposition pass. The contour shows tension down the centerline of the bead at the end of every pass. This tension is mainly due to thermal effects during bead cooling, with some contribution from the phase transformations of the build plate below the weld.

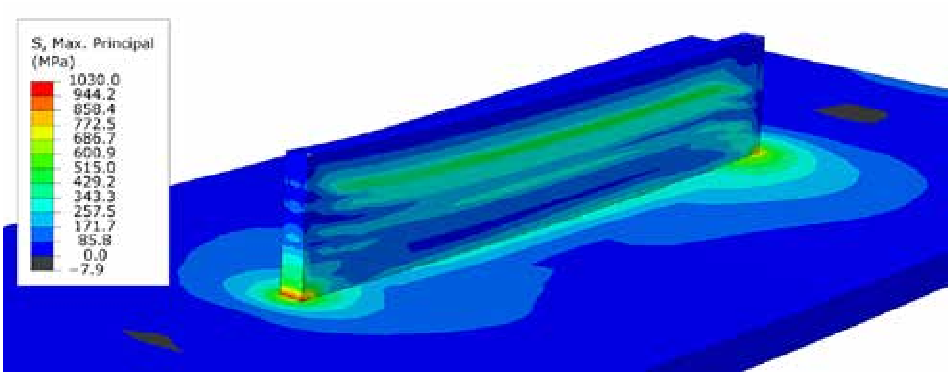

Figure 3: Max principal stress after the final deposition pass and cool to room temperature.

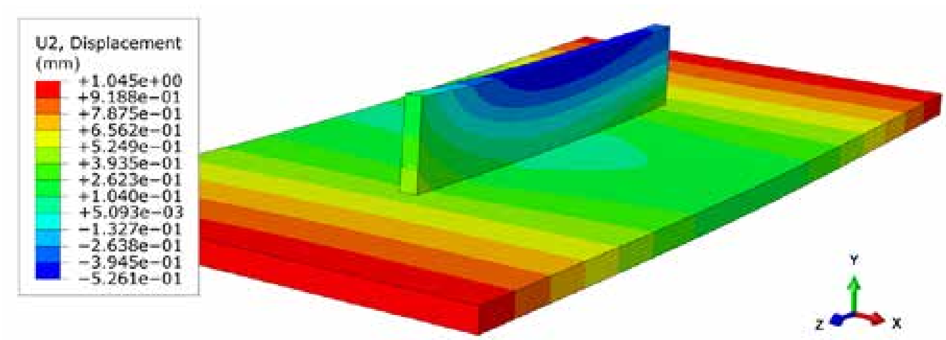

Figure 4: Vertical displacement at the end of the process after cooling to room temperature.

As subsequent passes build on top of each other, the previous passes are stress relieved and retransformed to austenite. Figure 2 shows in-process stresses halfway through pass five, with the tensile stresses being relieved ahead of the deposition. As the material is being deposited, there is tri-axial compression caused by the volume expansion of the material being heated. Also, there exists some compression behind the heat-affected zone along the build path. This compression can be explained by the solid-state phase transformation from austenite to ferrite and pearlite, and the associated volume expansion.

At the end of the process, tension and neutrality dominates the built wall, while tri-axial compression is almost nonexistent. The contour in Figure 3 shows how the stress gradients differ from pass to pass. Small neutral bands separate the tension pass-by-pass which gives the wall a tiger-striped appearance. High magnitudes of tension also reside in the corners where the first deposition layer attaches to the build plate. This high level of tension may cause the build to prematurely detach from the plate during the process, or even warp the build plate. Some additive manufacturing builds rely on this tension to easily separate the plate from the build, where differing materials, with different coefficients of thermal expansion, aid in the separation after reheating and quenching.

Finally, the distortion contour, Figure 4, shows the ends of the build plate curl up in the deposition direction after the process, while the wall dips slightly in the center. The model predicts about one millimeter of curl on each end of the plate, which is due to the cycles of thermal expansion in the center forcing the plate ends out and up. The dip in the center of the build is exaggerated by the bow in the build plate and is mainly due to the overheating caused by the deposition as each pass evolves.

The shrinkage is at a minimum at the start of each pass and increases as the wall heats up. At first, the thermal energy from each pass is quickly transferred to the wall and build plate, but as the wall temperature increases the heat transfer slows.

CONCLUSIONS

A thermal and stress model was successfully developed to simulate the wire arc additive manufacturing process, with the assistance of QustomWeld to help with the complicated events of the process and to setup the Goldak torch parameters, coupled with DANTE's material and phase transformation models to predict in-process and residual stress, phase evolution, and distortion.

Additive manufacturing is becoming more reliable as processes are developed and refined. The models developed from this study, and the previous study, illustrate the challenges inherent to the WAAM process and shed light on issues that can be avoided before the first bead is even deposited. These results include the overheating shown from the thermal model and relatively high levels of tension shown in the stress model.

Distortion is also a huge concern if high-tolerance parts are to be manufactured. Industry moves so fast that there exists a culture of "print it and then find out" but, using analytical tools, build issues can be teased out before they become manufacturing headaches.

REFERENCES

[1] Meyer, Jason M. "Using Welding Simulation Tools to Model WAAM." Thermal Processing, 15 Sept. 2022.

[2] QustomApps: https://www.qustomapps.com/

ABOUT THE AUTHOR

Jason Meyer joined DANTE Solutions full time in May 2021 after receiving his master's degree in mechanical engineering from Cleveland State University. His main responsibilities include marketing efforts, project work, and support and training services for the DANTE software package and the DANTE utility tools. Contact him at jason.meyer@dante-solutions.com.

D. SCOTT MACKENZIE, PH.D., FASM
SENIOR RESEARCH SCIENTIST–METALLURGY /// QUAKER HOUGHTON INC.

The quench factor can be directly determined from the Jominy end quench as a function of distance from the quenched end.

Quench factor analysis: C-curve determination

Previously, I discussed the concept of the quench factor, as developed by Staley [1]. We showed that it was possible to determine properties as a function of quench rate using the Jominy end quench. In this column, I will discuss the C-curve and the determination of the coefficients of the C-curve.

INTRODUCTION

The C-curve is like the Time-Temperature-Transformation curve for continuous cooling. In general, the C_t function is described as [1]:

$$C_t = K_1 K_2 \left[exp\left\{\frac{K_3 K_4^2}{RT(K_4 - T)^2}\right\} \exp\left\{\frac{K_5}{RT}\right\}\right]$$

where C_t is the critical time required to precipitate a constant amount of solute. The meaning of each of the constants are described in my previous article.

To determine the parameters K_1, K_2, K_3, K_4, and K_5, it is first necessary to have the C-curve. C-curve data is scarce and of limited availability. Some Time-Temperature-Property curves have been collected [2]. Some coefficients for the C_t function are shown in my previous column and in [3]. Once the C-curve, or Time-Temperature-Property curve, is obtained, the values of the coefficient are obtained by repeated iterations (and minimum error) until the best fit to the C-curve is achieved [4].

DETERMINATION OF THE C-CURVE

From the above discussion, the quench factor, τ, can be determined for any position on the Jominy end quench with hardness measurements. Since the quench factor is related to the C-curve by the relationship:

$$\tau = \int \frac{dt}{C_t}$$

Or:

$$\tau = \frac{\Delta t_1}{C_1} + \frac{\Delta t_2}{C_2} + \frac{\Delta t_3}{C_3} + \ldots\ldots + \frac{\Delta t_n}{C_n}$$

In the Jominy end quench, an infinite number of quench rates are available, and the path is known from the relationship described by [5]. It is important to understand that the cooling rates can change due to the changes in thermal conductivity of aluminum due to alloying content.

Based on this relationship, the time increments, Δt_1, Δt_1, Δt_3, through Δt_n, can be determined by examining the quench path, and dividing the critical temperature range (400°C through 200°C) into intervals at specific temperatures. Since the C-curve is independent of the quench path, a series of nonlinear equations can be established to solve for the critical time, C_t for different quench factors:

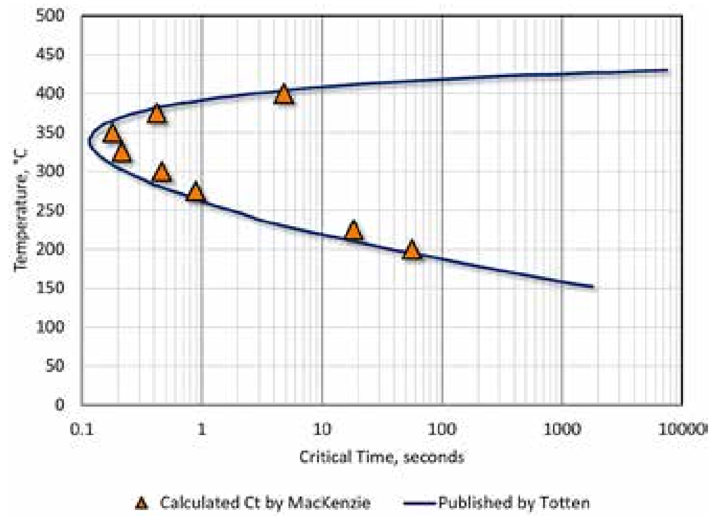

Figure 1: 7075-T6 C-curves determined from Jominy end quench [11] compared to previously published C-curve [12] [13].

$$\tau_1 = \frac{\Delta t_1}{C_1} + \frac{\Delta t_2}{C_2} + \frac{\Delta t_3}{C_3} + \ldots\ldots + \frac{\Delta t_n}{C_n}$$

$$\tau_2 = \frac{\Delta t_1}{C_1} + \frac{\Delta t_2}{C_2} + \frac{\Delta t_3}{C_3} + \ldots\ldots + \frac{\Delta t_n}{C_n}$$

$$\tau_3 = \frac{\Delta t_1}{C_1} + \frac{\Delta t_2}{C_2} + \frac{\Delta t_3}{C_3} + \ldots\ldots + \frac{\Delta t_n}{C_n}$$

$$\tau_n = \frac{\Delta t_1}{C_1} + \frac{\Delta t_2}{C_2} + \frac{\Delta t_3}{C_3} + \ldots\ldots + \frac{\Delta t_n}{C_n}$$

where τ_1, τ_2, τ_3. ... τ_n are the quench factors from locations on the Jominy end quench specimen; Δt_1, Δt_1, Δt_3, through Δt_n are the temperature intervals from the quench path at specific locations on the Jominy end quench, and C_1, C_2...C_n are the critical times on the C-curve.

Solution of this set of equations will provide the C-curve, or critical time as a function of temperature. To minimize false and unrealistic answers, it is necessary to constrain the results of the solution to the series of nonlinear equations solved above. Examples of the constraints used are the stipulation that all solutions for C_t must be positive and not equal to zero. Further, the results are constrained to yield results C_t less than 5,000. Examination of the data available [4] [6] [7], indicates that this is a reasonable assumption. Better solutions for the shape of the C_t curve would be obtained with more nonlinear equations.

Gandikota [6] provides a program for the simultaneous solution

to the above equations. Once the C-curve is obtained, calculation of the constants K_2, K_3, K_4, and K_5 is difficult, because of the very non-linear nature of the equations. However, the use of thermodynamic data as suggested by Shuey and Tiryakioglu [7] [8] simplify analysis. Further improvement can be achieved by the implementation of the improved quench factor model of Rometsch [9] or Tiryakioglu [7] [8].

Problems with the equation for the C-curve are its complex nature and dependence on K_2–K_5. Different sets of K_2–K_5 can provide similar fits to the data, with similar errors, but can provide wildly different Time-Temperature-Property curves [7]. Fitting the Time-Temperature-Property coefficients is severely non-linear, and results in errors regardless of the method used. Independent physical data offer much better fits to the data and result in reduced errors in the C-curve. Data such as the solvus temperature (K_4), solute diffusivities (K_5), and enthalpy for precipitation (K_7) substantially reduce the fitting errors and non-linearity and offer physical meaning to the data and fit. Use of the thermodynamic data also drastically reduces the computational load. Use of many data points (> 10) reduces the errors. Combining interrupted quench data and continuous cooling data is very effective in reducing C-curve errors.

An example of such a solution is shown in Figure 1. The data fit published data well, within the constraints cited by others [9] [10] [7]. This data demonstrates the usefulness of the technique and is a powerful tool to be used for the prediction of properties resulting from changes in heat treatment.

CONCLUSIONS

In this short column, we have described a method of determining the C-curve for aluminum, using the Jominy end quench. From the C-curve, we can calculate the coefficients in the C_t function, and then be able to calculate properties. Since properties are also a direct function of the quench rate, the quench factor can be directly determined from the Jominy end quench as a function of distance from the quenched end, or quench rate in the critical range of 400°C through 200°C.

Should you have any suggestions for additional columns, or have questions regarding any column, please contact the editor or myself.

REFERENCES

[1] J. T. Staley, “Quench Factor Analysis of Aluminum Alloys,” Mat. Sci. Tech., vol. 3, p. 923, November 1987.

[2] H. Chandler, Ed., Heat Treater's Guide: Practices and Procedures for Nonferrous Alloys, Materials Park, OH: ASM International, 1996.

[3] D. S. MacKenzie, “Metallurgy of Heat Treatable Aluminum Alloys,” in Heat Treating of Nonferrous Alloys, vol. 4E, G. E. Totten and D. S. MacKenzie, Eds., Materials Park, OH: ASM InternationAL, 2016, p. Metals Handbook 2A.

[4] J. W. Evancho and J. T. Staley, “Kinetics of Precipitation in Aluminum Alloys During Continuous Cooling,” Met. Trans., vol. 5, pp. 43-47, January 1974.

[5] G. P. Dolan, R. J. Flynn, D. A. Tanner and J. S. Robinson, “Quench factor analysis of aluminum alloys using the Jominy end quench technique,” J. Mat. Sci. Tech., vol. 21, no. 6, pp. 687-692, 2005.

[6] V. Gandikota, “Quench Factor Analysis of Wrought and Cast Aluminum Alloys, PhD Dissertation,” 2009.

[7] R. T. Shuey, M. Tiryakioglu and K. B. Lippert, “Mathematical Pitfalls in Modeling Quench Sensitivity of Aluminum Alloys,” in Proc. 1st Intl. Sym. Metallurgical Modeling for Aluminum Alloys, 13-15 Oct. 2003, Pittsburgh, PA, 2003.

[8] M. Tiryakioglu and R. T. Shuey, “Multiple C-Curves for Modeling Quench Sensitivity of Aluminum Alloys,” in Proc. 1st Intl. Sym. Metallurgical Modeling for Aluminum Alloys: 13-15 October, 2003, 2003.

[9] P. A. Rometsch, M. J. Starink and P. J. Gregson, “Improvements in Quench Factor Modeling,” Mat. Sci. Eng., vol. A339, pp. 255-264, 2003.

[10] R. T. Shuey and M. Tiryakioglu, “Quenching of Aluminum Alloys,” in Quenching Theory and Technology, B. Liscic, H. Tensi, L. C. Canale and G. E. Totten, Eds., Boca Raton, FL: CRC Press, 2010, pp. 43-84.

[11] D. S. MacKenzie, Quench Rate and Aging effects in Al-Zn-Mg-Cu Aluminum Alloys, PhD Dissertation, Rolla, MO: University of Missouri - Rolla, 2000.

[12] G. E. Totten, G. M. Webster and C. E. Bates, “Quenching,” in Handbook of Aluminum: Volume 1 Physical Metallurgy and Processes, G. E. Totten and D. S. MacKenzie, Eds., Boca Raton, FL: Marcel Dekker, 2003, p. 975.

[13] G. E. Totten, C. E. Bates and L. M. Jarvis, Heat Treating, p. 16, December 1991.

ABOUT THE AUTHOR

D. Scott MacKenzie, Ph.D., FASM, is senior research scientist-metallurgy at Quaker Houghton. He is the past president of IFHTSE, and a member of the executive council of IFHTSE. For more information, go to www.quakerhoughton.com.

TONY TENAGLIER
HEAT TREAT PROCESS ENGINEER ///
HITCHINER MANUFACTURING

To establish employee value beyond a paycheck, look for potential, recognize motivators, and balance rewards to keep process moving forward.

Employers need to expand on carrot-stick philosophy

We all trade time for money. Gone are the days of bartering, trading your chickens for goats. We go to work to earn a paycheck. Making money is important. That is how a company stays afloat and how employees make money to live. But it is also important to understand another meaning of "value" for employees, to motivate them to perform the necessary work.

ESTABLISHING VALUE

There is a classic image of a donkey looking at a carrot dangling just in front of his nose as he pulls a cart forward that depicts the classic "extrinsic" motivation model — place a nice juicy carrot in front of employees and they will pull whatever load is required to get the reward. But to fully understand what is actually going on in the performance of employees, it's necessary to realize it must be something beyond the mere placement of a "carrot" in front of them that motivates them to put parts into a furnace, reduce scrap costs, and get parts to the customer on time.

THE DONKEY

The first component of this metaphor is that the donkey has to be competent. We would not designate a bird to pull the necessary cart with a carrot in front. This isn't to say that employees are donkeys (though donkeys are actually hard-working). The problem, though, is that sometimes the donkeys aren't a good fit and maybe the donkey acts out in a way of displeasure. So, like a coach in football, employees must be placed in their areas of strength and talents. Some athletes are best suited for a linebacker, others a quarterback or a kicker. It's the same in heat treat, where some strengths of the operators will depend on their interests, backgrounds, and professional goals. Although all of the operators performing the work in heat treat can do the basic skills of setting up, running, and reviewing a completed cycle, there are other areas of skill such as pyrometry, furnace tuning, and even metallurgical evaluation that can also provide motivation to get the work done.

Some heat-treat operators like to know more about "why" they are pulling the cart, such as what does heat treat do to the microstructure? Other operators are more concerned about the quality of the cart they are pulling. Or they might be interested more in how the furnace is properly calibrated or how to tune the power settings to achieve the temperature uniformity required for cycles.

THE CART

The second component is the relationship of the donkey to the cart — the employee to the work they are assigned to do. The cart is the work

All employees want to test their skills in some shape or form. To make the claim that people simply "work for a paycheck" is overlooking an important aspect of what else is also motivating someone to do what they do. Any carrot needs to be juicy enough for employees to want to work toward it. It also has to actually be given to them in intervals that keep them on the path toward the company's success.

to be performed. The furnace that needs to be loaded. The cycle that has to be quickly turned around into a deep freeze and eventually tempered. Can the employee move the cart? Do they have the skills to do this? Is the cart setup in a way they can actually get the work done?

If the cart is too heavy, the employee won't be able to get the work done. Too many cycles running at the same time might cause errors in load setup and even cycle completion. If the cart is too light, production might suffer and a bottleneck occurs where parts aren't being full processed.

The cart represents the minimum work that needs to get done. Sometimes to push the employee, simply dumping the work on them without telling them does not turn out well and they will get nowhere. Instead, the goal for managers in heat treat should be to set up the scenario where the employees want to load their cart each day and perform the necessary work.

THE CARROT

The third component is the actual carrot, representing what employees are chasing after. This extrinsic reward is often the focal point of reward systems in performance review systems of employees. However, it overlooks a critical component of intrinsic motivators of employees. All employees want to test their skills in some shape or form. To make the claim that people simply "work for a paycheck" is overlooking an important aspect of what else is also motivating someone to do what they do. Maybe they want to be the best at understanding metallurgical phenomena in the way of a football quarterback striving to be the best quarterback. What is sometimes hard to accept is that American work culture sometimes overlooks the fact that some people simply can enjoy the work they do. So, employees default to sayings such as, "I'm just here for a paycheck" or "It's just a job." And, yes, they are and it is, but there are many types of work — other options — out there. If they are sticking around, it's not only the pay that is keeping them there at this point.

But the carrot needs to be juicy enough for employees to want to work toward it. It also has to actually be given to them in intervals that keep them on the path toward the company's success. If the carrot is dangling in front of them forever and just used as a constant teaser, the employee will give up and the cart will stop there.

CONCLUSION

One of my greatest satisfactions as the heat-treat process owner has been getting new employees with no familiarity with material science and educating them to understand and be able to explain the phenomena of microstructure evolution during heat treat. It is also in developing each employee to the fullest potential of what they can do in their position. I have seen employees with a high-school education excel at the materials science portion. I have seen employees with minimal automation engineering backgrounds excel in the tuning of PID and power settings. The trick to establishing value beyond a paycheck is to see the potential of each employee, recognize the cart they are pulling and what they might want to carry on it for work to get done, and to balance the carrot placed in front to keep the process continually moving forward.

ABOUT THE AUTHOR

Tony Tenaglier is the heat treat process engineer at Hitchiner Manufacturing. He earned both a B.S. in material science engineering and an M.A. in psychology. You can contact Tenaglier at tony_tenaglier@hitchiner.com.

A NEW LOW-PRESSURE CARBURIZING SOLUTION

IN A PIT VS. TRADITIONAL PIT CARBURIZING METHODS

Pit LPC is a new and revolutionary furnace system that is a drop-in replacement for traditional atmosphere pit carburizing solutions.

By THOMAS HART

Pit Low Pressure Carburizing (LPC) for case hardening of large gears is a new approach to a traditional technology. Today's manufacturing environment demands process, quality, and environmental improvements. Heat-treatment applications can have an extremely large impact in the reduction of overall costs and time. LPC of gears have been traditionally conducted in horizontal batch configurations with disadvantages that include the limitation of maximum gear size produced deterring the idea of LPC for large gears. Vertical designs allow for the maximum use of a furnace working volume; however, it comes with its own challenges. Vertical LPC oil quench designs are demanding as they must be connected vertically (requiring a tall shop height and pit for quenching). Vertical vacuum furnaces with high pressure gas quenching (HPGQ) can be used; however, quenching in gas has its limitations vs. oil quenching. Traditional atmosphere pit carburizing designs offer unwanted (yet accepted) effects, including a flammable atmosphere, cumbersome atmospheric generators, intergranular oxidation, etc. The pit LPC approach allows LPC to take place safely and environmentally friendly in a vacuum-heating chamber. Upon the conclusion of the boost/diffusion cycles, the component(s) can be removed from the heating chamber and placed into a separate oil quench vestibule. Typical LPC furnaces do not allow this as degradation of internal materials take place when exposed to oxygen. The pit LPC design has a heating system that can operate under vacuum and can be exposed to oxygen during material transfer to quench. Deep case depths require long carburizing cycle times, especially at lower temperatures, whereas the benefits of pit LPC design allows carburizing at higher temperatures such as 1,800-1,900°F (980-1,040°C) reducing the carburizing times drastically (up to 50 percent) compared to lower temperatures, saving operating costs and case hardening times.

INTRODUCTION

Modern case hardening by carburizing, a practiced method to surface harden steel, is reaching its centennial anniversary. Although case hardening within carbon environments (pack carburizing) was practiced prior to the 20th century, modern case hardening received its notable start in the 1920s. Now, 100 years later, there are several different methods to introduce carbon to austenitized ferrous metal surfaces, increasing the carbon concentration at the surface by the diffusion of carbon toward the core, creating the case-hardened carbon profile. Austenitized steel is a phase transformation of steel at elevated temperatures above 1,340°F [725°C] and allows higher levels of carbon to be absorbed into the steel surface. These carburizing methods include:

- Pack carburizing.
- Liquid (salt bath) carburizing.
- Gas carburizing.
- Low pressure carburizing (LPC).

The ending result of these methods provides a hard and wear resistant surface with a soft and/or tough core for low carbon steels and does not have a high degree of hardenability. These processes are conducted in heat-treatment furnaces of varying designs, shapes, and sizes.

Modern carburizing heat-treatment furnaces can be produced in continuous, semi-continuous, and batch type, and they can be provided in horizontal, vertical, and rotary configurations. Manufacturing volumes, component geometry, material grade, variety of geometries, and material grades all influence the optimum furnace type and configuration. Material grade and cross sections can drastically influence the design based on how intense the quenching media is needed to obtain the desired hardness. Since carburizing is typically conducted on low carbon and, due to its low hardenability, the cooling process must be rapid to prevent the austenite transformation back to ferrite/pearlite in the core. Higher carbon steels typically do not require as aggressive of a cooling process, and slower quenching media can be used.

Carburizing case depths vary drastically depending on the size and demand a component is going to be subjected to. The required carburizing case depth directly affects the duration of the carbon boosting. The deeper the case depth, the longer the carbon boost and diffusion stage will be while at the austenitizing temperature. When deep case depths are required, extremely long furnace process times are required when carburizing in the 1,700°F (925°C) range. For example, 0.08" (20 mm) requires approximately 12 hours whereas 0.15" (3.8 mm) requires approximately 36 hours. When carburizing at lower temperatures, the diffusion of carbon takes place much slower and can take up to twice as long.

In general, when small working volumes and low weights are required, small horizontal furnace configurations are typically used. Contrast this to large heavy loads, and the large vertical furnace configuration becomes the preferred method of heat treatment. Since these large components tend to be quite heavy, overhead crane material handling typically is the preferred method of material transfer, and the furnace hearth can be optimized to accommodate the large masses. It is also worth noting that comparing the working volume of a horizontal furnace to a pit furnace, the pit furnace will be less costly to manufacture, in addition to having the ability to handle greater mass per working volume. Pit-furnace hearths can be constructed to handle much greater load masses since they are loaded via an overhead crane system vs. bottom supported loads as in horizontal furnaces.

When manufacturing requires carburizing on large diameter components or components that are long and narrow, the chosen furnace configuration often will be a pit type. Long components typically require hanging during heat treatment as horizontally supporting them often leads to sagging and deformation. Long components either can be large and bulky (with small volume loads) or small in diameter (with large volume loads). It is common for large components that require carburizing to have deep case depths; this means that components will be in the furnace for long durations keeping the furnace occupied and not able to process additional loads. Considering that deep case depths on large components tie up the furnace for long durations, manufacturers are driven to heat treat as many components in a furnace as possible, affecting the need for the furnace to handle loads with heavy masses and large geometric footprints.

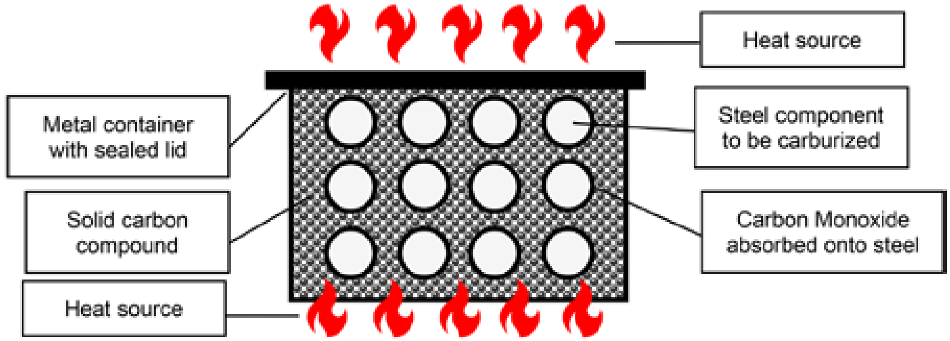

Figure 1: Pack Carburizing Setup (example).

CARBURIZING METHODS

Pack Carburizing

Pack carburizing is one of the earliest forms of carburizing, and it provides the addition of carbon to a steel component via a decomposition of a solid compound in a sealed metal container as illustrated in Figure 1.

Pack carburizing processes higher temperatures than that of gas and liquid carburizing and does not have the ability to directly quench the carburized components, which are enclosed in the steel container with solid carbonaceous compounds. This process is very challenging to control, produces non-repeatable results, requires an additional core refinement process (due to large grains and slow cooling), and a case refinement process. Therefore, pack carburizing is not commonly practiced due to its labor intensiveness, lack of process control and environmental issues, giving way to liquid and gas carburizing methods.

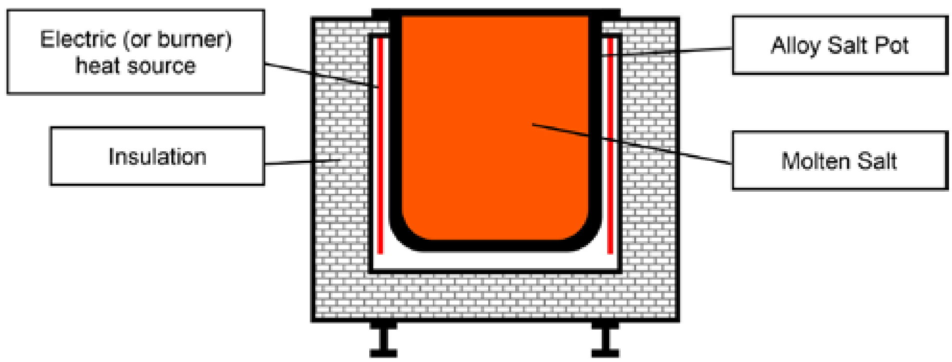

Figure 2: Liquid (salt bath) carburizing furnace (example).

Liquid (salt bath) Carburizing

In liquid carburizing, steel components are submerged in a molten-salt bath and held at temperatures above a material's austenitic transformation range. The salt bath, sometimes referred to as a chloride bath, consists of sodium cyanide (the carbon source), barium chloride, and sodium chloride. The decomposition of these salts at high temperatures causes the carbon to decompose near the austenized steel surface and diffuse into the steel. Also note that nitrogen can sometimes diffuse into the surface in addition to the carbon. Salt bath heating operates in the 1,560-1,650°F (850-900°C) range for shallow cases and 1,650-1,750°F (900-950°C) range for deeper cases. Salt baths provide excellent temperature control, rapid heat transfer, and allows for direct quenching after carburizing. Figure 2 illustrates a typical construction of an electrically heated salt bath furnace using a high-temperature alloy salt pot to contain the molten salt.

Salt-bath carburizing, like pack carburizing, is not a commonly practiced carburizing method in modern industry, and with salt-bath processing, it derives several disadvantages. When at higher temperatures, the degradation of the salt bath and furnace components happens at accelerated rates, requiring the replenishment of salt and constant furnace maintenance. Due to the decomposition of the salt, a "sludge" forms and requires constant removal and recharging of the salt composition. Part washing is required after quenching, and, due to residual salt adhering to the component when hot and in the salt bath, liquid carburizing is not recommended for components that have geometric features such as threads, slots, and/or small holes. Additionally, the residual salt remaining on a component will contaminate the quenching media.


Figure 3: Pit furnace.

Figure 4: Box (integral quench) furnace.

Figure 5: Continuous furnace.

Figure 6: Rotary furnace.

Gas Carburizing

Gas carburizing, developed in the 1950s, became a favored technique due to the unreliable methods of pack carburizing and the associated issues with liquid carburizing. Currently, gas carburizing is the most widely used type of carburizing in modern industry. A wide variety of conventional furnaces including pit, box, continuous, and rotary types are used for gas carburizing and as in any heat-treating process,

Figure 7: Endothermic gas generator.

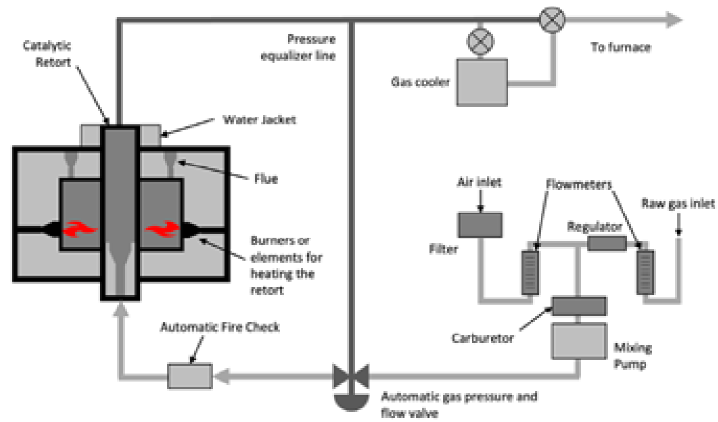

Figure 8: Endothermic gas generator schematic piping arrangement [4].

the proper choice of furnace design depends largely on component geometry, total production demand, and production flow. Figure 3 through Figure 6 provide types of atmosphere furnaces equipped for carburizing.

In gas carburizing, the carbon source, typically natural gas (or propane), composed largely of methane, is introduced to the furnace via an inert carrier gas such as nitrogen. The carbon and nitrogen sources are monitored and mixed external to the furnace in endothermic generator systems where the gasses pass through a heated retort containing a nickel catalyst, see Figure 7 and Figure 8. When the mixed gas leaves the retort, it is quickly cooled to prevent the reformation of carbon into soot and is sent to the furnace so the carbon can then diffuse into the steel. [3]

In comparison to pack or liquid carburizing, gas carburizing and its carbon potential allows deeper and higher carbon content cases to be obtained more rapidly.

"Carbon potential of a furnace atmosphere at a specified temperature is defined as the carbon content of pure iron that is in thermodynamic equilibrium with the atmosphere. The carbon potential for the furnace atmosphere must be greater than the carbon potential for the surface of the workpieces in order for the carburizing to occur. It is the difference in the carbon potential that provides the driving force for the carbon transfer to the parts." [1]

This advantage is due to the carbon potential of the gas environment in the furnace being higher than that of the steel, and when the temperature of the steel is at 1,700°F (925°C), the surface of the steel is highly active and allows the surplus carbon in the atmosphere to diffuse into the surface. Increasing the temperature drastically affects the diffusion rate of carbon into austenite, for example 1,700°F (925°C) is approximately 40 percent faster than 1,600°F (870°C).

DISADVANTAGES OF GAS CARBURIZING

Carburizing at 1,700°F (925°C) happens to be the most common carburizing temperature. Due to atmospheric furnace construction characteristics, higher temperatures will generate excessive deterioration, especially in the thermally resistant alloy materials. Due to the furnace's limitation to exceed 1,700°F (925°C), there is no significant way to speed up the diffusion rate of carbon into austenite.

In its early years, gas carburizing proved to be a process that was difficult to control as it relied on operators removing "shim stock" from within the furnace, weighing them as the process continued to assess how much carbon had been absorbed, which translated to the active case depth of the charge within the furnace at the time of its removal. At the time of gas carburizing, beginning operators were required to measure these shims at various stages of the process to ensure the desired carbon absorption was achieved. There were challenges associated with the measurement of "shim stock" as it was a continuous and labor-intensive monitoring process that ultimately led to inconsistent results from batch to batch. These inconsistencies and industries' demand for more precise and reliable results led to the introduction of the oxygen probe atmosphere monitoring process. The oxygen probe gave the furnace the ability to measure the residual oxygen within a furnace's atmosphere, which subsequently identifies the carbon potential of the atmosphere. [5]

However, control of the carbon potential for a given carburizing process is complex. Multiple systems are required (Figure 8) to create the proper atmosphere and dew-point control. Water vapor in the furnace atmosphere directly affects carbon potential, and control of dew point is critical to the success of carburizing. The catalyst within the endothermic generator will deplete over time, requiring monitoring and replacement when the reaction is insufficient. Excessive sooting within the catalyst will affect its performance and will require a burnout.

When a furnace has been idle for an extended period or has recently completed a soot removal burnout, the amount of new enriching gas needed to maintain a given carbon potential of an empty furnace is found to be much higher than would be expected. As time passes (typically 12-24 hours), the amount of enriching gas required to maintain the carbon potential decreases to a steady state value. This is a process called "furnace conditioning" and is the time that carbon is attracted to low temperature locations such as crevices and brickwork. However, as the furnace continues to operate, there are some locations in the furnace system where soot will continue to deposit such as sight ports and gas sample lines, which, over time, will affect the furnace's carburizing capability. [1]

Gas-carburizing atmospheres are highly toxic and highly flammable and form explosive gas mixtures when mixed with air. A safety program emphasizing furnace operator training and preventative maintenance should be established and adhered to for all heat-treating operations using controlled atmospheres. Atmosphere gas discharged from the furnace to the operating environment must be burned to ensure poisonous carbon monoxide is converted to carbon dioxide. Pilot flames must always be maintained on atmosphere vent lines, and there must be a flame curtain that ignites automatically whenever a furnace door opens. [1]

Intergranular oxidation (IGO) takes place when steel is exposed to oxygen atoms at elevated temperatures. Oxygen is present from the process gas decomposition, and it then diffuses slowly into the steel-grain boundaries. This oxygen diffusion combines chemically with the existing elements that favor reactions with the oxygen.

Figure 9: Vacuum furnace.

Figure 10: Two chamber vacuum oil quench furnace and loader [7].

Advancements in automotive and aerospace designs now more than ever are looking to LPC as its go-to case-hardening solution for transmission components.

IGO is observed as microscopic cracks in a material's surface up to approximately 0.006" deep but can be larger due to carburization time, temperature, and gas composition. In atmosphere furnaces, formation of IGO is not preventable, and its removal must be done via grinding, hard machining, polishing, or other mechanically suitable process. The only other way to eliminate IGO is to provide the heat-treatment process within an oxygen-free environment via low pressure carburizing (LPC). In this case, a vacuum furnace removes the oxygen present within its chamber via a vacuum pumping system prior to the start of heating.

Despite gas carburizing's ability to monitor the temperature and gas composition, it still suffers from numerous limitations including

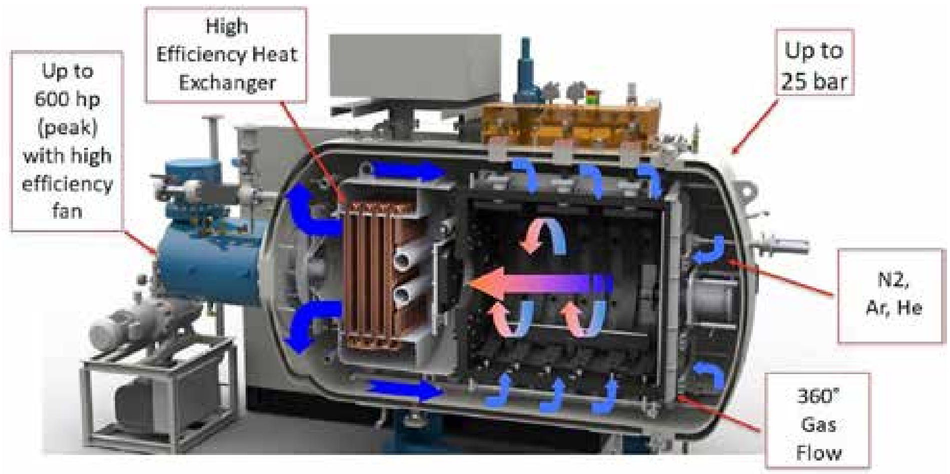

Figure 11: Key features of a vacuum furnace with HPGQ.

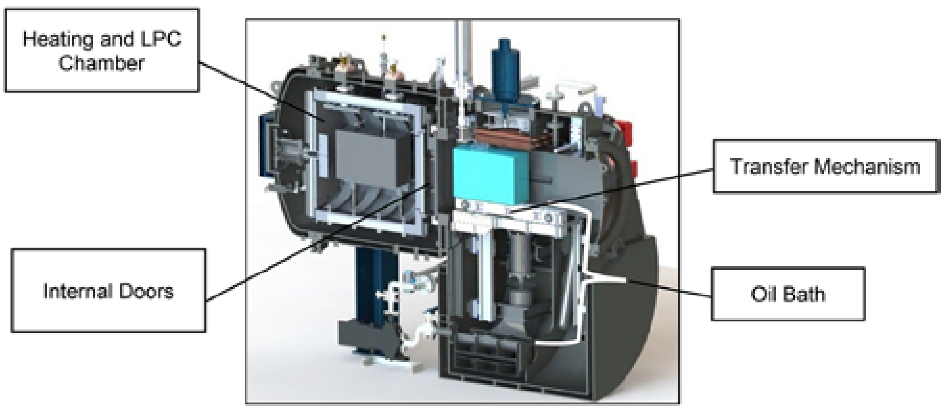

Figure 12: The key quenching features of a vacuum oil quench furnace.

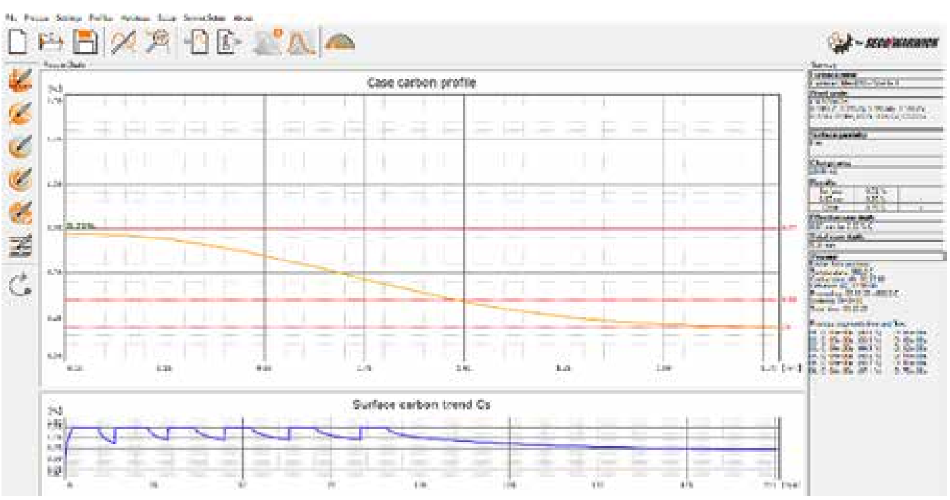

Figure 13: Example LPC simulator summary screen.

the furnace equipment itself, hazardous operations, inconsistent case depths, and IGO. Industry, as a result, searched for an improved method of carburizing, leading to the invention of LPC.

LOW PRESSURE CARBURIZING IN VACUUM FURNACES

LPC differs from atmosphere gas carburizing. As its name suggests, it takes place at pressures below atmospheric pressures (low pressure) requiring the process to be carried out in a vacuum furnace instead of atmospheric furnaces. LPC found its origins in the 1970s where early users introduced propane as the carbon source to the process. Propane generated heavy sooting within the furnace, which led to arcing among the internal heating system if not properly maintained. This drove industry to further improve upon the process. In the 1990s, the introduction of acetylene as the carbon gas proved to have the desired chemical reaction of hydrocarbon gasses at low pressures without the unwanted effects of sooting. This was due to the steel's ability to catalyze and decompose acetylene's carbon molecules diffusing them into its surface. [5]

LPC process consists of loading a charge in the vacuum furnace; the door is then closed, and the vacuum pumping system begins removing oxygen from the chamber. Once the proper vacuum level is reached, the heating system is turned on and heats the charge to the desired austenization temperature, typically between 1,660-1,750°F and then LPC can begin. The LPC process consists of a series of acetylene boosting and diffusion segments where the acetylene is precisely introduced to the heating chamber via mass flow controller(s) at approximate pressures of 8 torr [10 mbar] then followed by a diffusion segment where the boosted carbon, which has saturated the steel surface, diffuses toward the materials core. This cycle is repeated with varying times and segments as needed to achieve the desired effective case depth (ECD). The alternating segment pattern is needed as the catalytic decomposition (or cracking) of the acetylene takes place much faster than the diffusion of the carbon into the steel [5]. Once the ECD is achieved, and depending on alloying elements, the charge can either be directly quenched in HPGQ or in oil or the furnace can be lowered in temperature to 1,500-1,550°F for material stabilization prior to quenching.

Vacuum furnaces can also be provided in multiple configurations similar to traditional atmospheric furnaces such that they can be manufactured in continuous, semi-continuous, and batch types along with horizontal and vertical configurations. As previously mentioned, in other carburizing techniques, vacuum furnace configuration also depends on manufacturing volumes, component geometry, and material grade. Vacuum furnaces can be provided with various quenching media as well. Most common LPC vacuum furnace constructions are a single chamber batch system equipped with the required acetylene LPC gas flow system and high-pressure gas quenching (HPGQ) represented in Figure 9. This furnace type is suited for alloys that have the hardenability for quenching in HPGQ. When alloy hardenability cannot be quenched in HPGQ, a multi-chamber vacuum oil quench furnace can be used. Figure 10 illustrates a horizontal multi-chamber vacuum oil quench batch furnace.

Another advantage of an LPC vacuum furnace is that horizontal batch system referenced in Figure 9 can be equipped with gas quenching at pressures up to 25 bar. Quenching pressures up to 25 bar with quenching gas distribution nozzles arranged at 360 degrees around the furnace hot zone and in the front door provide a less aggressive quench than that of oil, providing the necessary hardness, all while minimizing distortion. Figure 11 illustrates the major components of a HPGQ furnace that can include a high-power quenching blower (up to 600 HP), high efficiency heat exchanger, and an ASME certified pressure vessel to contain the required quenching gas pressure. Gasses typically used include nitrogen, helium and/or argon, depending on process requirements.

When a steel alloy requires a faster quenching requirement, an LPC system can be employed on a multi-chamber vacuum oil quench furnace. In this system, the heating chamber and quenching chamber are isolated from one another. In a double chamber solution, a charge is placed in the quenching vestibule on a transfer mechanism, and the external door is closed. Once both chambers are pumped down and oxygen is removed, the internal pressure and thermal doors are opened for charge transfer between chambers. The charge is then heated to austenization temperature and the LPC can begin. Upon the completion of the LPC process, the internal chamber doors open, and the material transfer system retrieves the charge, returning it to the oil quenching chamber and submerges the charge into the oil to complete the hardening process.

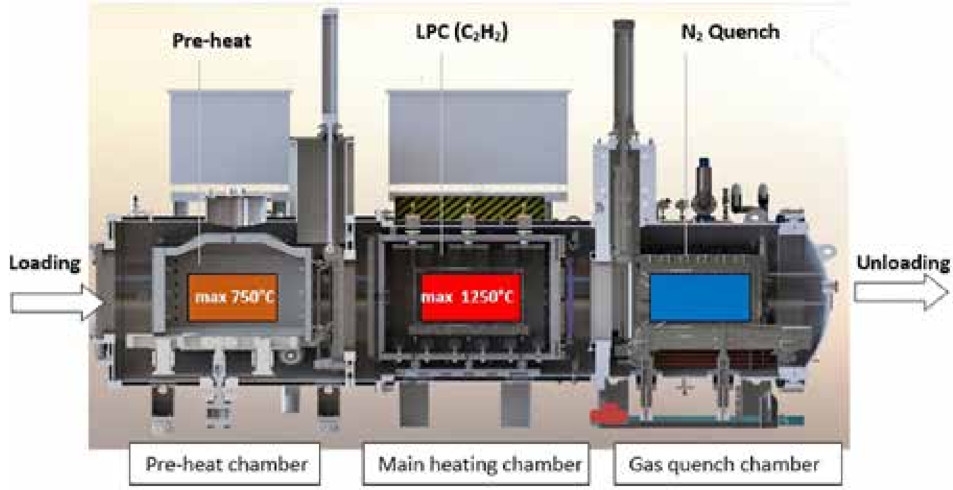

Figure 14: Semi-continuous (three chamber) vacuum HPGQ furnace [6].

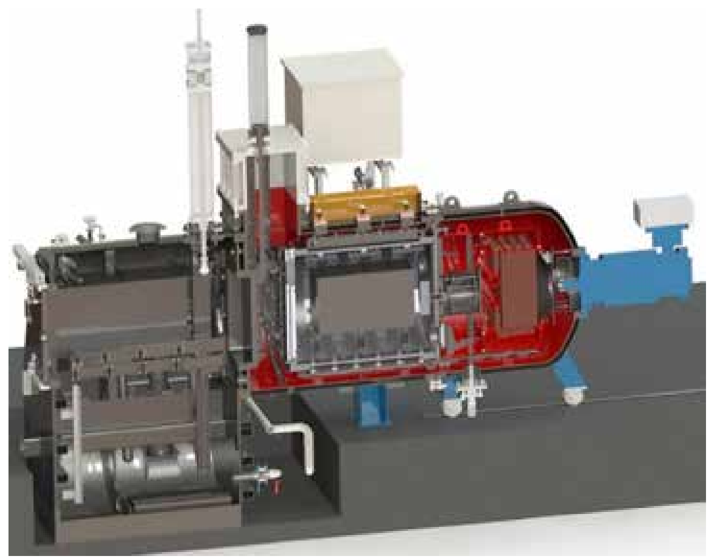

Figure 15: (Two chamber) vacuum furnace with HPGQ and Oil [6].

Figure 16: Single-piece flow vacuum furnace with LPC and with part dedicated HPGQ chamber [7].

ADVANTAGES OF LOW PRESSURE CARBURIZING IN VACUUM FURNACES

Traditional atmosphere furnaces for carburizing have limitations on maximum operating temperature due the materials used for insulating and heating. Their temperature ranges are typically limited to 1,700°F (925°C) whereas typical vacuum furnaces have temperature ratings up to 2,400°F (1,310°C). This is due to oxygen being removed from the furnace via the pumping system, thus preventing the reaction of oxygen and its degrading effects to the insulation and heating elements. With this ability of the vacuum furnace to heat past 1,700°F (925°C), carburizing cycle times can be dramatically reduced due to the steel's ability to absorb and diffuse carbon at much higher rates. LPC provides fast, effective, efficient, uniform, and precise carburizing for regular or densely loaded charges and difficult shaped parts. The process time can be reduced up to five times depending on carburizing temperature, in comparison to traditional carburizing drastically reducing the overall processing time and utility costs.

The continuous development and advancement of LPC has brought on the implementation of sophisticated process modeling and control methods (Figure 13) allowing LPC to be a direct replacement of gas carburizing in those industries, which require case hardening of its components.

Simulation software provides the ability to develop and simulate the carburizing processes prior to running a process. The simulation algorithm performs calculations based on steel grade, temperature, size and shape of parts and carburized surface area to return the optimized sequence of carburizing and diffusion stages, as well as predicted carbon profile within the parts. The boost and diffusion sequences can be imported to the furnace recipe management system, which eliminates the potential for human error in data entry.

Advancements in automotive and aerospace designs now more than ever are looking to LPC as its go-to case-hardening solution for transmission components. Industry is placing more strict demands on material performance and, as a result, base materials are being updated to enhance their material characteristics. LPC is a perfect solution for legacy and upcoming demands, and where applicable,

Figure 18: Pit furnace.

Figure 19: Typical pit carburizing quench tank [6].

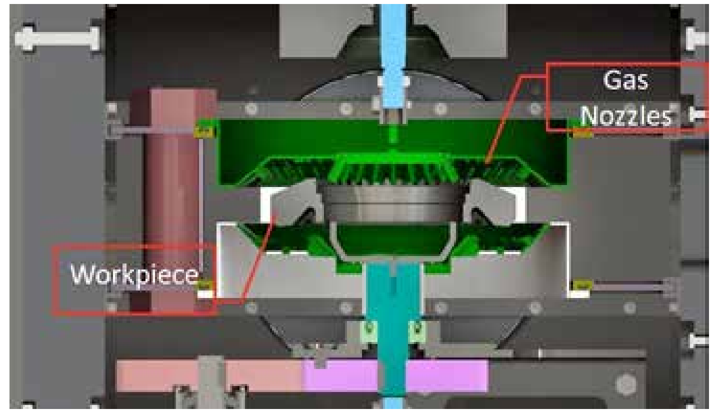

Figure 17: Part dedicated HPGQ chamber with manifold and rotational hearth [7].

HPGQ can be the preferred choice of quenching media, as it brings less distortion to that of oil quenching.

Not only are there single-chamber and double-chamber vacuum furnaces, but vacuum furnaces can also be configured in various other multi-chamber solutions. Those include Figure 14 through Figure 17, which further show the advancement in carburizing.

Additional advantages of LPC in a vacuum furnace compared to traditional gas carburizing with oil quenching include:

- Decreased distortion.
- Elimination of intergranular oxidation (IGO).
- No decarburization.
- Elimination of endothermic generators.
- High productivity.
- High accuracy and repeatability of carbon penetration.
- Reduction of carburizing time.
- Lower process costs.
- Excellent case uniformity.
- Unlimited carbon transfer.
- Guaranteed process repeatability.
- No CO_2 emission.
- Environmentally-friendly.

Not only do these advantages pertain to the aerospace and automotive industries, but they also apply to industries such as energy, tool and die, and medical [5].

ATMOSPHERE PIT CARBURIZING

Historically, atmosphere pit carburizing has been the chosen method for carburizing of large, long, and heavy work pieces. As mentioned in the introduction, this is primarily due to the pit furnace's heavy loading capacity with tall working envelopes. The furnaces will be stand-alone systems (Figure 18) that have an accompanying quench tank next to the furnace (Figure 19).

In pit furnace systems, the load is typically supported on a fixture transported by an overhead handling system (often a crane) from material staging, then to the furnace, from the furnace to the quench tank (Figure 19) and from the quench tank to post processing such as the washing system. When transferring from the furnace to the quench tank, it provides a hazardous work environment due to the intense heat radiation being emitted from the load and fire risk if the load is quenched in an oil bath [5]. Additional and adverse problems associated with pit carburizing include:

- Long process times.
- A flammable atmosphere (endogas and methane).
- Maintenance of costly furnace components such as retorts and circulating fans.
- Furnace conditioning.

Gas Carburizing @ 1700°F (925°C) Cycle Steps
Heat up to 1560°F (850°C)
Soak at 1560°F (850°C)
Heat up to 1700°F (925°C)
Carburize
Cool to 1500°F (820°C)
Oil Quench
Temper at 360°F (180°C)

Table 1: Base parameters of the atmosphere carburizing process.

LPC @ 1800°F (980°C) Cycle Steps
Heat up to 1800°F (980°C)
Carburize
Cool and soak at 1500°F (820°C)
Oil Quench
Temper at 360°F (180°C)

Table 2: LPC carburizing process description at 1,800°F (980°C)

LPC @ 1900°F (1040°C) Cycle Steps
Heat up to 1900°F (1040°C).
Carburize
Cool and soak at 1500°F (820°C)
Oil Quench
Temper at 360°F (180°C)

Table 3: LPC carburizing process description at 1,900°F (1,040°C).

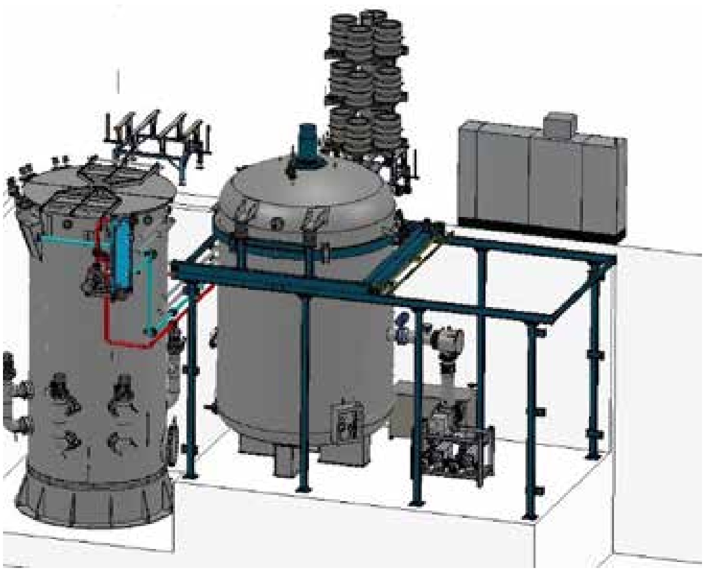

Figure 20: Pit-LPC system model [5].

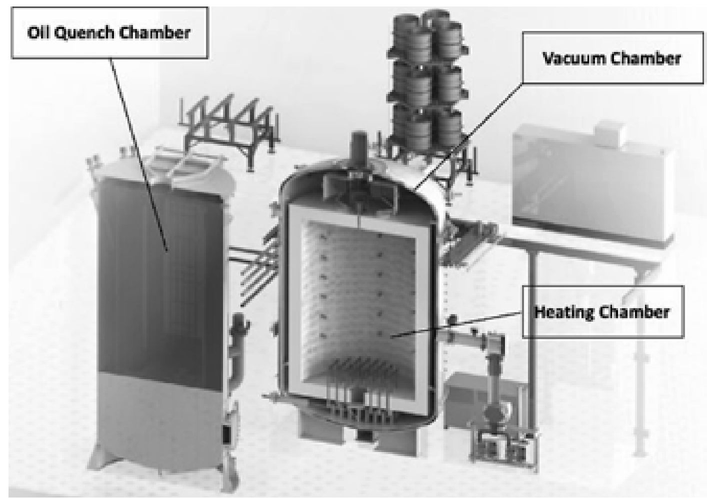

Figure 21: Cross section Pit-LPC system.

Figure 22: Pit-LPC furnace.

» Process monitoring (using sample coupons or continuous monitoring devices).

» Presence of intergranular oxidation.

» Furnace conditioning.

These disadvantages prove there is a need for changes to the traditional pit carburizing approach. LPC is that alternative that includes a safe working environment, no CO_2 emissions, and shortened process times; however, it had not been offered pit configurations until now.

THE PIT LPC FURNACE SYSTEM

Pit LPC provides a new and innovative approach bringing together the traditional cold wall design of a vacuum furnace with rod style metallic heating elements that are incorporated into a ceramic fiber lining, while making it possible for them to resist oxidation when exposed to oxygen at high temperatures. Note, this system does not include an alloy retort. A traditional graphite-lined vacuum furnace does not have the ability to be exposed to air as the graphite oxidizes immediately as it reacts with oxygen when at elevated temperatures. Since the Pit LPC furnace includes the necessary insulating and heating components that resist oxidation, once the LPC process is completed, the furnace can be opened (while at the LPC temperatures), and the hot load can be removed and transferred to its adjacent quench tank as illustrated in Figure 20 through Figure 22 [5]. Additionally, the furnace is equipped with a water-cooled heat exchanger and quench fan, which means a load can be slow cooled if a rapid oil quench is not required.

The furnace system reference here has the stand-alone furnace system with LPC and an adjacent quench tank and includes the following features:

» Working zone of 70” (1,800 mm) diameter 120” (3,000 mm) depth.

» Gross load mass of up to 17,600 lb. (8,000 kg).

» Heating power of 360 kW.

» Maximum temperature of 2,012°F (1,100°C).

» Integrated vacuum pumping system.

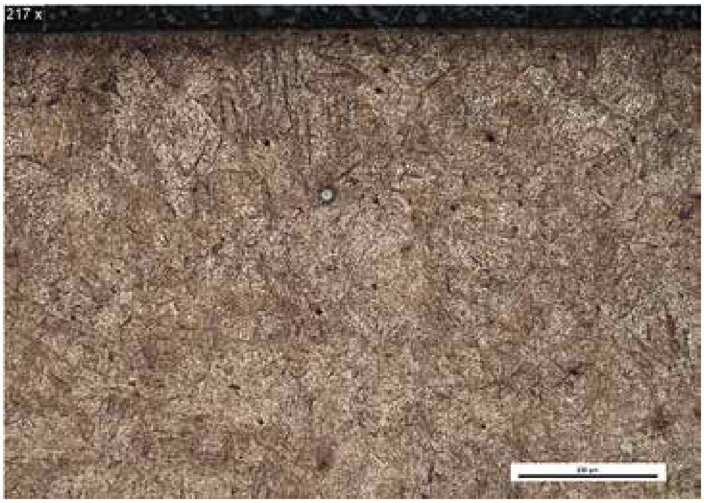

Figure 23: A micrograph of the resulting microstructure, which consists of martensite and approximately 10 percent retained austenite (100x magnification).

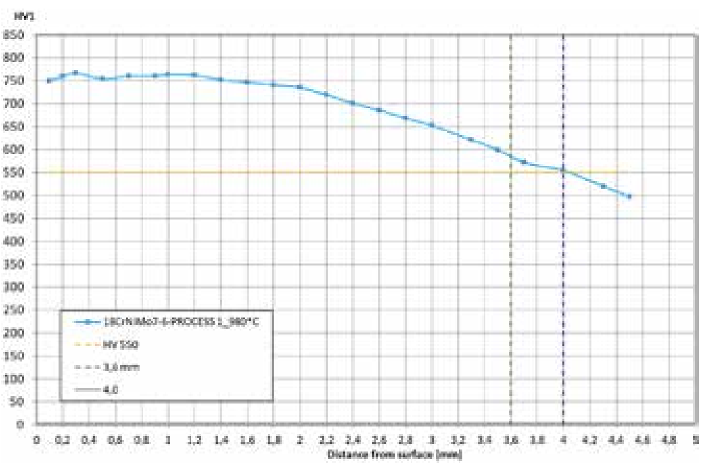

Figure 24: The hardness profile resulting from the 1,800°F (980°C) LPC process.

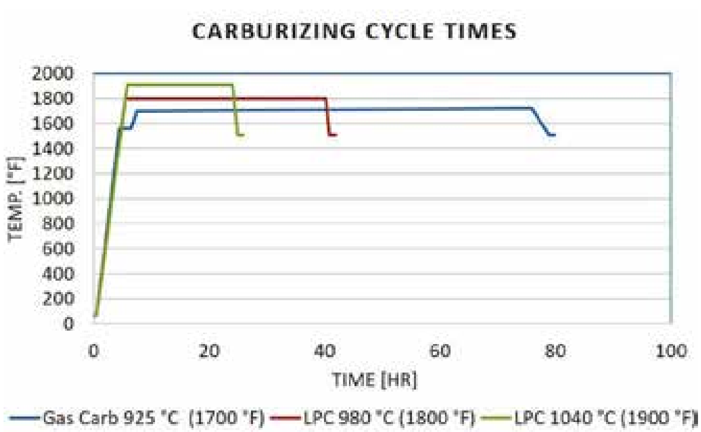

Figure 25: The carburizing cycle times resulting from the proposed carburizing cycles.

» 10^{-2} torr (10^{-2} mbar) vacuum range.

» Acetylene as the carbon source gas and includes an LPC process simulator.

» To limit distortion, forced nitrogen cooling is also included for a more rapid temperature drop before quenching.

PIT LPC CASE STUDY

To highlight the advantages in using a Pit LPC furnace system for carburizing large and heavy parts, a case study was completed on a load with the following characteristics [5]:

- **Mass:** 13,230 lb. (6,000 kg).
- **Steel Grade:** SAE 4820 (18CrNiMo7-6).
- **Desired Effective Case Depth (ECD):** 0.157" (4.0mm) at 50 HRC.
- **Carburized Surface Area:** 215 square feet (20 square meters).
- **Carburizing Temperature:** 1,700°F (925°C).

This load was simulated in both a gas-carburizing cycle in a traditional atmosphere pit type furnace and LPC in the Pit-LPC system. The comparison is based on both an atmosphere gas carburizing furnace at a plant and LPC data retrieved in the laboratory Pit Style-LPC furnace. The steps used in the gas carburizing cycle are shown in Table 1.

In contrast to the base atmospheric carburizing process, an LPC process was simulated at two different temperatures to understand the effect of carburizing temperature on the cycle time. The corresponding LPC cycle steps are shown in Table 2 for 1,800°F (980°C) and Table 3 for 1,900°F (1,040°C).

Table 3 then shows the LPC cycle steps used at 1,900°F (1,040°C).

Process Parameter	ATM PIT	PIT LPC	
Carburizing Temperature (°F)	1,700	1,800	1,900
Duration (hr.)	80	42	26
Energy use (kWh)	8,100	3,787	3,124
Nitrogen use (scf)	3,530	4,207	3,050
Acetylene (scf)	0	483	483
Natural gas (scf)	10,594	0	0
CO_2 emissions (metric tons)	0.59	≈0	≈0

Table 4: Utility use resulting from the proposed carburizing cycles.

Process Parameter	ATM PIT	PIT LPC	
Carburizing Temperature (°F)	1,700	1,800	1,900
Duration (hr.)	80	42	26
Energy cost (kWh) ($0.127/kWh)	$1,028.70	$480.95	$396.75
Nitrogen cost (scf) ($0.0032/scf)	$11.25	$13.41	$9.72
Acetylene cost (scf) ($0.169/scf)	0	$81.60	$81.60
Natural gas cost (scf) ($0.00356/scf)	$37.72	0	0
Total utility cost	$1,077.67	$575.96	$488.07

Table 5: Utility cost resulting from the proposed carburizing cycles.

PIT LPC CASE STUDY – RESULTS AND ANALYSIS

All three carburizing processes were combined with an oil quench and temper where all three processes yielded similar metallurgical results. The micrograph in Figure 23 illustrates the resulting structure that is martensite with approximately 10 percent retained austenite [5].

The microstructure shown in Figure 23 is paired with the hardness profile measured on Figure 24 and shows the surface hardness reached nearly 62 HRC (770 HV) and ECD was 0.157" (4 mm) as defined by a 52.5 HRC (550 HV). Noteworthy, the grain size maintained appropriate ASTM size of 7. This profile was the result of the

Process Parameter	ATM PIT	PIT LPC	
Carburizing Temperature (°F)	1,700	1,800	1,900
Duration (hr.)	80	42	26
LPC process duration compared to gas carburizing	100%	52%	33%
Annual Processes (6500 hr./yr.)	81	155	250
Productivity Improvement	100%	190%	308%
Total cycle utility cost	$1,077.67	$575.96	$488.07
LPC utility costs compared to gas carburizing	100%	53%	45%
CO_2 emissions (metric tons)	0.59	≈0	≈0

Table 6: Summary of the potential productivity and savings of the Pit LPC system vs. gas carburizing in an atmosphere pit furnace on a per cycle basis.

Annual Processes	ATM PIT	PIT LPC
155	 Carb. Temp: 1700°F Total Cost: $166,782 CO_2 Emissions: 91.5 metric tons	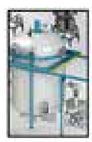 Carb. Temp: 1800°F Total Cost: $89,136 CO_2 Emissions: ≈0 metric tons
250	 Carb. Temp: 1700°F Total Cost: $269,417 CO_2 Emissions: 147.5 metric tons	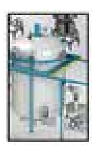 Carb. Temp: 1900°F Total Cost: $122,017 CO_2 Emissions: ≈0 metric tons

Table 7: Summary of the potential annual savings of the Pit LPC vs. gas carburizing in an atmosphere furnace.

1,800°F (980°C) LPC process [5].

To reach the hardness profile shown in Figure 24, the cycle profile is represented in Figure 25 (1,800°F). It is important to note that gas carburizing conducted at 1,700°F (925°C) cycle requires nearly 80 hours to complete. Meanwhile, LPC conducted at 1,800°F (980°C) required only 42 hours to complete, which is almost a 50 percent reduction. A further increase in carburizing temperature to 1,900°F (1,040°C) reduced the time to 26 hours, which is a 68 percent reduction, Figure 25 (1,900°F).

The reduced cycle time produced by the Pit Style-LPC drastically reduced the utility consumption while eliminating carbon dioxide and carbon monoxide emissions. The utility consumption in Table 4 shows an energy savings of 53 percent when LPC is employed instead of atmosphere gas carburizing. As such, when increasing the carburizing temperature while using LPC results, the end result proved to show increased savings of 61 percent. It is important to note that LPC eliminates the need for natural gas and the corresponding CO2/CO emissions. The corresponding cycle utility costs shown in Table 5 shows that switching to LPC has the potential of a 47 percent savings. An increase in the LPC temperature yields an even higher savings of 54 percent [5].

Impressive cost savings are not the only benefit to the Pit Style-LPC. Time savings also resulted in increased productivity vs. gas carburizing. When evaluating a five-day operating week, the Pit Style LPC unit has the potential to be drastically more productive. If carburizing at 1,800°F (980°C), the reduction in cycle time has the possibility to nearly double the total number of annual cycles. When evaluating carburizing at 1,900°F (1,040°C), this triples the annual number of cycles. Table 6 shows the increase in productivity and the accompanying savings per cycle [5].

To further illustrate the Pit LPC savings compared to atmosphere carburizing, the Pit LPC system has availability of 6,500 hours annually. At 1,800°F (980°C) 155 cycles are achievable in one Pit LPC furnace, in contrast to the gas carburizing process, which requires two atmosphere pit furnaces. The total processing cost would amount to $166,782, while the Pit-LPC costs would only be $89,136. This is a total savings of $77,646.

Moving to the higher carburizing temperature 1,900°F (1,040°C), 250 cycles are achievable in one Pit LPC system, compared to three atmosphere pit furnaces for the same demand. Meanwhile, the annual cost savings increases to $147,400. Table 7 summarizes the data behind this process savings.

CONCLUSIONS

Pit LPC is a new and revolutionary furnace system that is a drop-in replacement for traditional atmosphere pit carburizing solutions. This approach can handle the same large and/or long loads with deep ECD while reducing the process time and utility costs. These benefits drastically increase the ROI when converting from atmosphere carburizing to LPC while eliminating carbon emissions associated with gas carburizing.

BIBLIOGRAPHY

[1] ASM International Handbook Committee, ASM Handbook Heat Treatment, Vol. 4, 1991

[2] Herring, D.H. "The History of Vacuum Carburizing: 1968-Present." Process and Controls Training, 20-22 August 2019, SECO/WARWICK Corp., Meadville, PA

[3] Herring, D.H. "Atmosphere Heat Treatment: Atmosphere | Quenching | Testing" Vol.2. Troy, MI., BNP Media II, 2015.

[4] ASM International, Materials handbook; Heat Treating, Cleaning and Finishing, 8th Edition", Vol. 2, 1964

[5] Marteeny, D. "Vacuum Carburizing in a Pit Style Furnace: A 21st Century Solution to Large Component Case Hardening" ASM International, 2021

[6] Marteeny, D. "Hardening 4.0: An Evolution in Quenching Explained." Industrial Heating Webinar. 4 June 2020. www.industrialheating.com/events/1192-hardening-4-0-an-evolution-in-quenching- explained.

[7] Hart, T. "True Single Piece Flow Case Hardening for In-line Manufacturing.", ASM Heat Treat Show 2017, 24-26 October 2017, Greater Columbus Convention Center, Columbus, OH.

ABOUT THE AUTHOR

Thomas Hart is Product Manager – Vacuum Furnaces at SECO/VACUUM.

A pit LPC furnace. (Courtesy: SECO/VACUUM)

MECHANICAL PROPERTIES AND THERMAL CONDUCTIVITY OF LIGHTWEIGHT AND HIGH-STRENGTH

CARBON-GRAPHITE THERMAL INSULATION MATERIALS

The creation of closed pores inside carbon-graphite insulation material can adjust its compressive strength and thermal conductivity in both directions, reducing its thermal conductivity and improving its mechanical properties.

By JUNCHAO HE, HAIHUA WU, LEI ZHONG, QIANG ZHONG, QIANG YANG, XICONG YE, ZHI LIU, and YI KANG

Thermal insulation composites are widely used in civil and military applications; however, it is difficult to achieve the synergy of multiple technical objectives such as lightweight, thermal insulation, high-pressure resistance, and high-temperature resistance by adopting traditional preparation techniques. In this study, a novel carbon-graphite thermal insulation material was rapidly prepared by exploiting the micro-thermal press additive manufacturing forming technology, and these multiple objectives were simultaneously achieved by introducing a large number of closed pores. It was found that the percentage of closed pores in the carbon-graphite insulation grew by increasing the forming density or the amount of thermosetting phenolic resin added, but the thermal conductivity increased in parallel with the compressive strength, while the addition of pre-covered expandable graphite was able to achieve the synergy of high-compressive strength and low-thermal conductivity. When the content of thermosetting phenolic resin was 25 wt%, forming density was 1.2 $g\cdot cm^{-3}$, and expandable graphite was clad twice, the prepared carbon-graphite insulation exhibited a closed porosity/porosity ratio, compressive strength, and thermal conductivity of 48.92%, 16.432 MPa, and 0.743 $W\cdot m^{-1}\ K^{-1}$, which has the advantages of lightweight, high compressive strength, heat insulation, and high-temperature resistance and has good prospects for industrial applications.

INTRODUCTION

In spacecraft thermal protection systems (TPSs), the connection between the external anti-insulation layer and internal cold structure of the airframe must be prepared using thermal insulation materials, which act as thermal insulation and load-bearing components [1,2,3]. The representative thermal insulation materials at present are porous fibers/ceramics, aerogels, carbon-carbon (C/C) composites, and carbon-graphite [4,5,6]. Wang et al. prepared a novel high-temperature vacuum insulation material consisting of a graphite felt core and a sealing layer via chemical infiltration (CVI), named pyrolytic carbon and impregnated silica sol. When the temperature increased from 500 to 1,200°C, the effective thermal conductivity reduced from 0.403 to 0.368 $W\cdot m^{-1}\ K^{-1}$. This material was applied in the TPS of launch vehicles [7]. Wu et al. prepared a high-density high-temperature insulation material, which exhibited a bulk density of 1.64 $g\cdot cm^{-3}$ and bending strength of 47.8 MPa after heat treatment at 2,100°C [8]. Carbon-graphite insulation materials (e.g. carbon felt and flexible graphite paper) are superior to other insulation materials in terms of their temperature resistance, oxidation resistance, production cost, and mechanical properties, yet remain inferior in terms of the thermal conductivity. Moreover, it remains challenging to achieve synergy between multiple functional objectives such as a low weight, thermal insulation, high-pressure resistance, and high-temperature resistance.

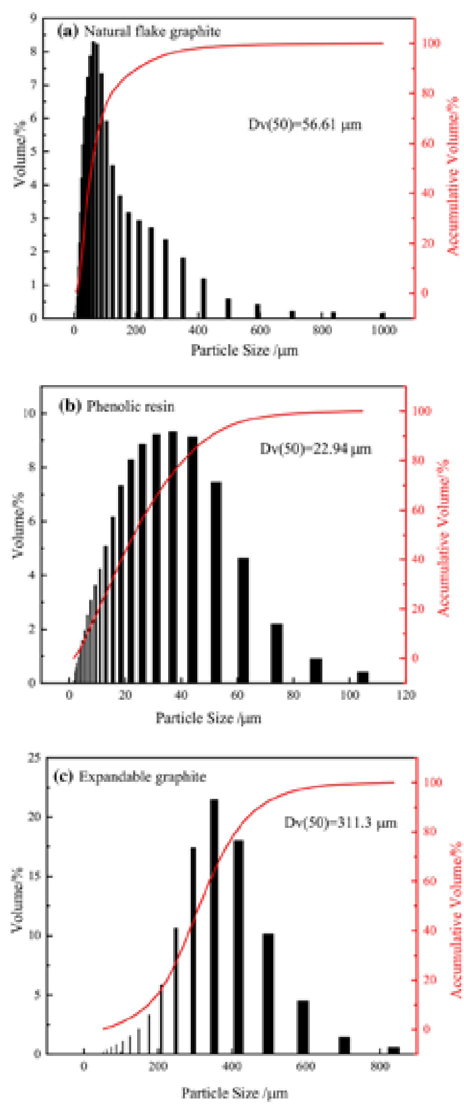

Figure 1: Particle size distribution of natural flake graphite, thermosetting phenolic resin and expandable graphite.

The introduction of closed pores in thermal insulation materials such as ceramics and carbon-graphite can effectively reduce their thermal conductivity while maintaining the mechanical properties. It was reported that a closed pore porosity of 14.5% can be attained by introducing microspheres with a content of 10%, and the thermal conductivity at 23°C can be reduced from 28.08 to 13.07 $W\cdot m^{-1}\ K^{-1}$ with a bending strength of 97.05 MPa [9]. Cheng et al. prepared porous mullite ceramics with a fully closed pore structure by direct solidification casting, using fly ash hollow spheres as the porogenic agent. The total porosity of this material ranged from 44.73-46.12%, with 99% of the pores being closed, and the compressive strength increased by 14.4% to 58.07±5.44 MPa [10]. Moreover, the research group used selective laser sintering to rapidly prepare a low-density carbon-graphite/silicon carbide composite thermal insulation material and noted that a certain number of closed pores could be formed inside the material through the addition of expandable graphite (200 mesh, 1–1.5 wt%). This framework simultaneously exhibited a low thermal conductivity and high compressive strength, with values of 1.21 $W\cdot m^{-1}\ K^{-1}$ and 13.87 MPa, respectively [11].

In this article, a new type of carbon-graphite thermal insulation material was prepared based on the principle of micro-thermal compression additive manufacturing technology. The effects of forming density, the amount of thermosetting phenolic resin added, and the number of times of cladding pretreatment on the pore state, compressive strength, and thermal conductivity of the charcoal-graphite thermal insulation material were studied, and the conditions and mechanism of closed pore formation were revealed. The thermal conductivity model and mechanical model were obtained by comparing the experimental data.

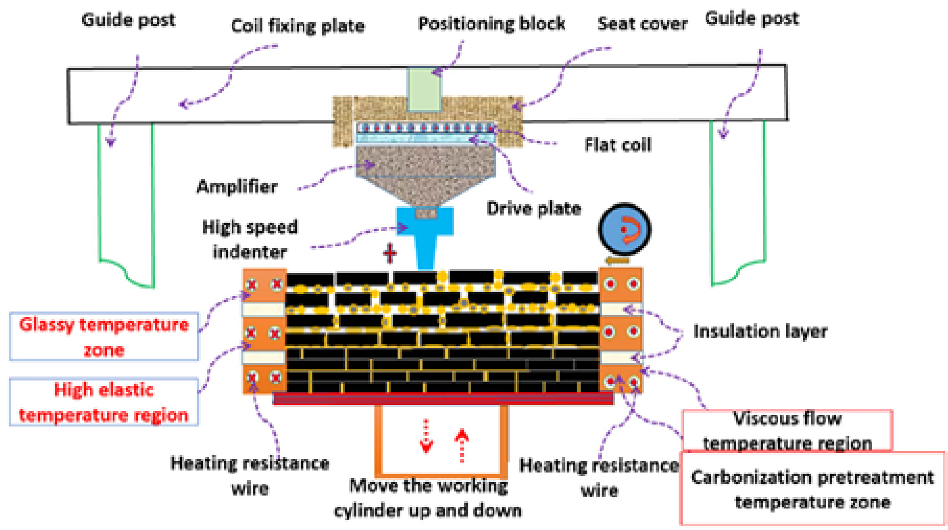

Figure 2: Principle diagram of the micro-thermal press additive manufacturing forming process.

Experimental materials	Natural flake graphite	Phenolic resin	Expandable graphite
Mass fraction (wt%)	74	25	1

Table 1: Mass ratios of thermosetting phenolic resin, natural flake graphite powder.

EXPERIMENT

Experimental materials

Natural flake graphite powder (99.5% carbon, D50=56.61 μm, supplied by Yichang Xincheng Graphite Co., Ltd.), thermosetting phenolic resin powder (SG-3130, D50=22.94 μm, supplied by Shanghai Aotong Industrial Co., Ltd.), and expandable graphite powder (99.5% carbon, D50=311.3 μm, supplied by Qingdao Xinghua Graphite Products Co., Ltd) were used.

Figure 1 shows the particle size distribution of natural flake graphite, thermosetting phenolic resin, and expandable graphite.

Materials	Mass fraction(wt%)					
Graphite	89	84	79	74	69	64
Phenolic resin	10	15	20	25	30	35
Expandable graphite	1	1	1	1	1	1

Table 2: Mass ratios of thermosetting phenolic resin and natural flake graphite powder.

Experimental procedures

Natural flake graphite, thermosetting phenolic resin, and expandable graphite were weighed in batches in a dry ball mill of type GQM (Xianyang Jinhong General Machinery Co., Ltd.) in established mass ratios and mixed well and then transferred to a micro-thermal pressing additive manufacturing forming system. The process can be summarized as follows: The graphite/phenolic resin/expandable graphite powder mix was laid flat, and, under the shear of the laying rollers, the natural flake graphite powder was deflected and oriented. The heated powder was rapidly struck in the selected area by using an electromagnetic indenter. The density of the billet was controlled by controlling the distance by which the indenter was lowered, and the compression of the powder layer was controlled by adjusting the speed of the indenter strike. The layers were stacked to obtain graphite-molded parts with a controlled density (Figure 2).

The prepared preform was placed in a vacuum sintering furnace for charring (evacuated to less than 100 Pa; ramped up to 300°C at 60°C/h and then ramped up to 800°C at 30°C/h for 1 hour, and cooled with the furnace), and the charred specimen was obtained.

The specimen preparation process was divided into three parts: (1) Variation in the forming density of the specimen. The uncoated expandable graphite was uniformly mixed with natural flake graphite powder and thermosetting phenolic resin powder according to the mass ratios listed in Table 1, and the micro-thermoforming system was used to prepare graphite pieces with forming densities of 1.0, 1.1, 1.2, 1.3, and 1.4 g·cm^{-3}, with five specimens for each group. (2) Variation in the amount of thermosetting phenolic resin added. The thermosetting phenolic resin powder and natural flake graphite powder were mixed evenly according to the mass ratios presented in Table 2, and specimens with a forming density of 1.2 g·cm^{-3} were prepared with five specimens for each group. The specific material ratios are listed in Table 2. (3) Pretreatment of the expandable graphite powder with coating. The expanded graphite was pre-treated using a boiling coating dryer (Changzhou Xinma Drying Engineering Co., Ltd.). (The coating solution consisted of 40 wt% liquid phenolic resin mixed with anhydrous ethanol at a mass ratio of 1:3, and the coating treatment was performed twice.) The expanded graphite was crushed after coating and sieved using a 200 mesh. The untreated expandable graphite, expandable graphite with one overcoating treatment, and expandable graphite with two overcoating treatments were mixed with natural flake graphite and thermosetting phenolic resin in accordance with the mass ratios listed in Table 1 to prepare specimens with a density of 1.2 g·cm^{-3}, with five specimens prepared for each group.

PERFORMANCE CHARACTERIZATION

To distinguish the types of pores, the bulk density and porosity of the specimens were tested according to GB/T 2998-2015 and international standard ISO 5016:1997, and the open porosity of the specimens was tested with reference to GB/T24529-2009. The closed porosity of the specimens was calculated as $P_\varepsilon = (1 - D_b/D_t \times 100\%) - P_\alpha$ (D_b is the bulk density of the specimens in g·cm^{-3}, D_t is the theoretical density of graphite, considered to be 2.256 g·cm^{-3}, and P_α is the specimen open porosity). The bulk density of the carbon-graphite heat insulation material specimen was calculated as $\rho = m/\upsilon$. Moreover, the compressive strength of the specimen was tested with reference to GB/T 13,465.3–2014, and the maximum compressive load of the specimen (Ø25 mm ± 0.1 mm) × (25 mm ± 0.1 mm) was determined using a WDW-100E micro-controlled electronic universal testing machine (provided by Jinan Kehui Experimental Equipment Co.). The arithmetic mean of the obtained experimental data was determined. (In the experiment, the indenter applied the load uniformly and with-

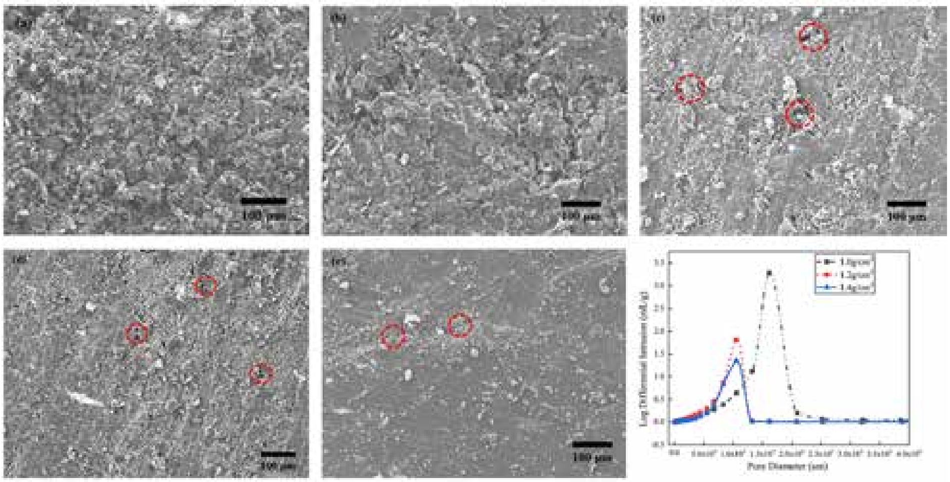

Figure 3: Microstructure of carbon-graphite insulation section and its pore size distribution at different forming densities a) 1.0 g cm^{-3}; b) 1.1 g cm^{-3}; c) 1.2 g cm^{-3}; d) 1.3 g cm^{-3}; e) 1.4 g cm^{-3}.

Density(gcm-3)	1.0	1.2	1.4
Total intrusion volume (mLg-1)	0.7467	0.4484	0.3199
Total pore area (m2g)	2.821	2.719	1.584
Median pore diameter (Volume,um)	1706.6	1031.1	1024.8
Median pore diameter (Area,um)	930	846.2	571.2
Average pore diameter (4 V/A,um)	1058.9	807.6	659.7
Porosity (%)	72.6452	58.7736	54.1115

Table 3: Structural properties of carbon-graphite insulation at different forming densities.

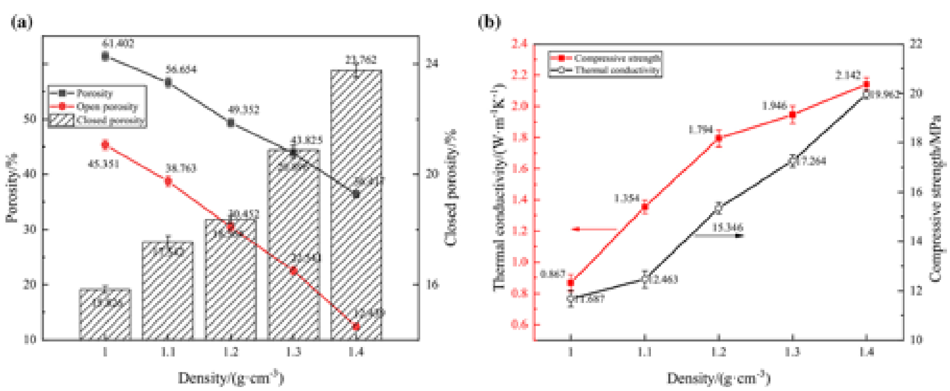

Figure 4: Effect of different forming densities on the properties of carbon-graphite insulation: a) porosity, open porosity, closed porosity; b) effect of compressive strength and thermal conductivity.

out impact at 15 mm/min, and the effective number of specimens for each group was 6.) The thermal conductivity of the specimens (Ø30 mm × 10 mm, six specimens in each group) was tested using a DRE-III thermal conductivity measurement instrument (provided by Xiangtan Xiang Yi Instrument Co., Ltd.). The specimens were transformed to optical sheets, and the JSM-7000F cold field emission scanning electron microscope was used to measure the thermal conductivity of the specimens. The aperture distribution and size of the specimens (10 mm × 10 mm × 10 mm) were evaluated using an AutoPore lv 9510 high-performance automatic mercury piezometer (supplied by Shanghai McMurray-Tick Instruments Co.)

RESULTS AND DISCUSSION

Effect of forming density on the properties of carbon-graphite insulation

Figure 3 shows the microscopic profile of a section of the carbon-graphite insulation material and its pore size distribution curve at different forming densities. Table 3 shows the test results of the mercury injection method. The average pore size of the carbon-graphite insulation was 1058.9 nm, 807.6 nm, and 659.7 nm at forming densities of 1.0, 1.2, and 1.4 g·cm^{-3}, respectively. The porosity decreased from 72.6452 to 58.7736% and 54.1115% as the forming density increased. This finding indicated that increasing the forming density led to a decrease in the number and size of pores within the carbon-graphite insulation.

Figure 4a shows the variation in the porosity, open porosity, and closed porosity of the carbon-graphite insulation material under different forming densities. As the density increased from 1.0 to 1.4 g·cm^{-3}, the porosity and open porosity decreased from 61.402% and 45.351% to 36.417% and 12.439%, respectively, and the closed porosity increased from 15.826 to 23.762%; moreover, the proportion of closed porosity gradually increased to 65.25%. In other words, increasing the forming density reduces the porosity of the carbon-graphite composite insulation and leads to the formation of more closed pores inside it. This phenomenon occurs because, during the micro-hot pressing process, the thermosetting phenolic resin becomes viscous and ensures the adhesion of the graphite powder and expandable graphite powder. Moreover, during the high-temperature carbonization process, the thermosetting phenolic resin undergoes a pyrolysis reaction, releasing CO_2, H_2, and water vapor (physicochemical process), and the H_2SO_4 and HNO_3 in the expandable graphite decompose into SO_2, CO_2, and a small amount of NO_x (Figure 5). When the forming density is low, owing to the low resistance, the gas generated can rapidly escape, leading to the formation of pores inside the carbon-graphite insulation. In this stage, the number of open pores is more. However, as the forming density continues to increase, gas discharge becomes more difficult. Part of the gas cannot be eliminated in time, leading to the formation of closed pores, and the number of closed pores increases. The continuous escape of gas during carbonization is the fundamental reason for the formation of pores within the carbon-graphite insulation, and the forming density directly influences the form of porosity.

Figure 4b shows the variation in the compressive strength and thermal conductivity of the carbon-graphite insulation material at different forming densities. Both the compressive strength and thermal conductivity of the material grew with the increase in the forming density. Specifically, as the density increased from 1.0 to 1.4 g-cm^{-3}, the compressive strength and thermal conductivity increased from 11.687 MPa and 0.867 W·m^{-1} K^{-1} to 19.962 MPa and 2.142 W·m^{-1} K^{-1}, respectively, corresponding to an increase of 70.81% and 1.47, respectively. This phenomenon occurred because, as the forming density of the preform increases, the graphite flake layer undergoes plastic deformation and orientation, leading to a stronger bond between graphite flakes, and the closed porosity increases [12]. At the same time, the vertical transmission of heat flow between carbon-graphite insulation materials changes from heat radiation to heat radiation and heat conduction, resulting in the increase of compressive strength and thermal conductivity of preforms [13].

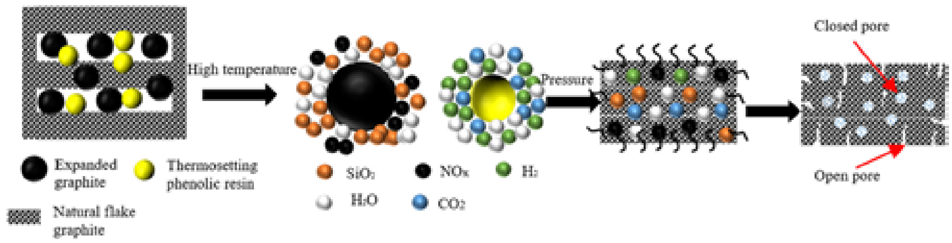

Figure 5: Schematic diagram of the mechanism of closed air pore formation.

Effect of thermosetting phenolic resin addition on the properties of carbon-graphite materials

Figure 6 shows the effect of the addition of thermosetting phenolic resin on the microscopic morphology of the carbon-graphite insulation material. In general, in the forming process of the micro-hot press additive manufacturing procedure, under the combined effect of the temperature field, shear force of the powder laying roller, and electromagnetic force, the natural scaled graphite powder is deflected and aligned along the direction perpendicular to the pressure, and the thermosetting phenolic resin is "distributed" as the binder. When the added content is low, the resin is mostly in the form of "lonely spots." At this time, there are a large number of pores inside the specimen, and the compressive strength and thermal conductivity are low, as shown in Figure 6a and 6b. When the added content is high, the molten thermosetting phenolic resin flows between the graphite flakes, filling the pores. Thus, the number of pores in the specimen gradually reduces, the microstructure becomes denser, and the graphite flakes are more flatly oriented (Figure 6c, 6d, and 6e). Consequently, the compressive strength, and thermal conductivity of the specimen increase with the addition of phenolic resin.

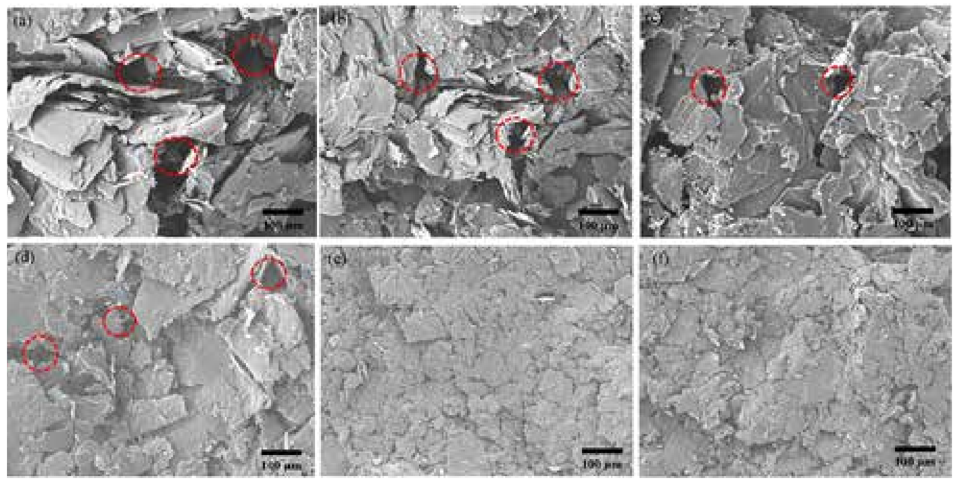

Figure 6: Effect of thermosetting phenolic resin addition on the microscopic morphology of carbon-graphite insulation; a) 10%; b) 15%; c) 20%; d) 25%; e) 30%; f) 35%.

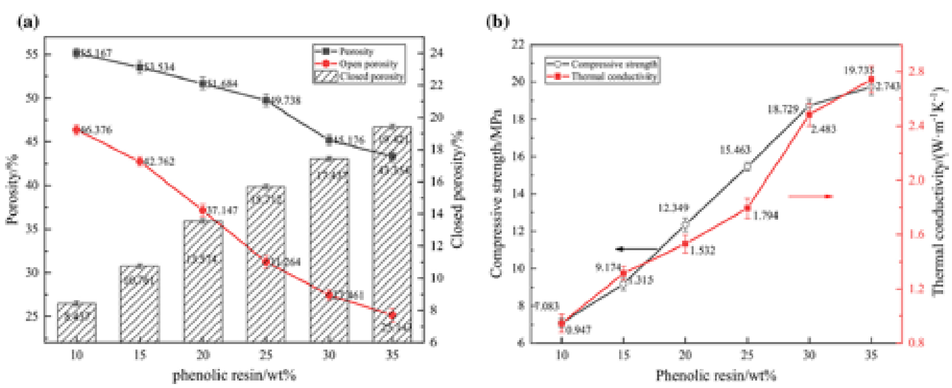

Figure 7: Effect of different thermosetting phenolic resin powder additions on the properties of carbon-graphite insulation: a) porosity, open porosity, closed porosity; b) effect of compressive strength, thermal conductivity.

Figure 7a shows the effect of the addition of different amounts of thermosetting phenolic resin powder on the porosity, open porosity, and closed porosity of the specimens. As the amount of added thermosetting phenolic resin powder increased from 10 to 35%, the porosity of the specimens decreased from 53.167 to 43.354%, and open porosity decreased from 46.376 to 25.143%, indicating that the closed porosity gradually increased. When the added content of phenolic resin powder was 35%, the closed porosity was the highest (19.421%), with a proportion of44.80%. This phenomenon occurs because as the amount of thermosetting phenolic resin added increases, a larger amount of thermosetting phenolic resin fills the gaps between the graphite sheets under the action of the micro-hot pressing forming temperature and pressure. During charring, a larger amount of gas escapes, forming more holes; however, the larger amount of resin char remaining (phenolic resin residual carbon rate is as high as 70–80%) fills the spaces between the graphite sheets, reducing the number of holes, and resin carbon shrinks by 2% volume at high temperatures. Moreover, the addition of more thermosetting phenolic resin makes it more difficult for gases to escape, leading to the formation of more closed pores inside the specimen. The combined result of these factors leads to a decrease in the total and open porosities of the carbon-graphite insulation [14].

Figure 7b shows the effects of addition of different amounts of thermosetting phenolic resin powder on the compressive strength and thermal conductivity of the charred specimens. The compressive strength and thermal conductivity increased with the addition of thermosetting phenolic resin powder. Specifically, when the amount of added thermosetting phenolic resin powder increased from 10 to 35wt%, the compressive strength increased from 7.083 MPa to 19.735 MPa and thermal conductivity increased from 0.974 $W \cdot m^{-1} K^{-1}$ to 2.743 $W \cdot m^{-1} K^{-1}$, corresponding to an increase of 178.62% and 189.65%, respectively.

In summary, although the increase in the forming density or amount of added thermosetting phenolic resin increases both the compressive strength and thermal conductivity, increasing the forming density has a more notable effect on the thermal conductivity

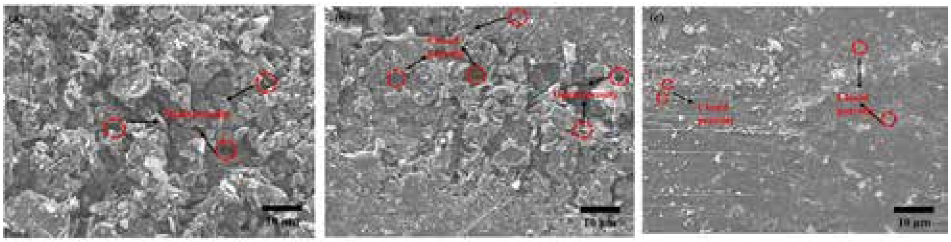

Figure 8: Effect of different wrapping times on the microstructure of carbon-graphite insulation: a) unwrapped; b) wrapped once; c) wrapped twice.

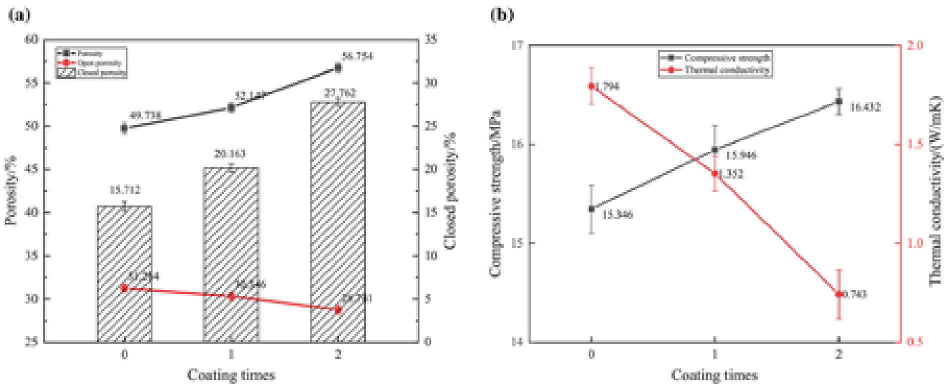

Figure 9: Effect of different cladding times on the properties of carbon-graphite materials: a) porosity, open porosity and closed porosity; b) compressive strength and thermal conductivity.

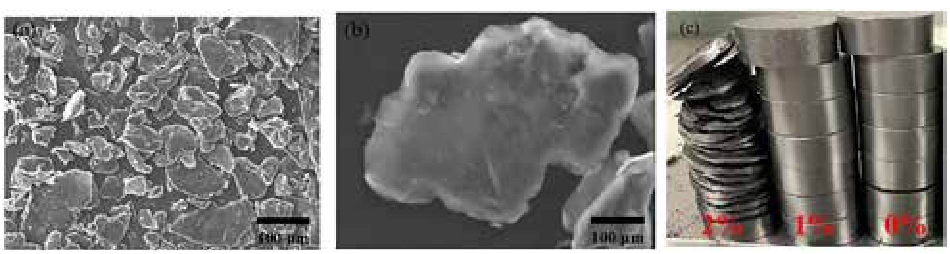

Figure 10: Microscopic morphology of expandable graphite cladding twice and state after carbonization (Figure 10c shows the different states of the carbon-graphite insulation after carbonization at three levels of 0%, 1% and 2% of expandable graphite addition, respectively).

of the carbon-graphite material and increasing the amount of the added thermosetting phenolic resin has a more notable effect on the compressive strength. Notably, in both cases, the closed porosity ratio of the carbon-graphite insulation material increases, owing to which the compressive strength and thermal conductivity simultaneously increase. In general, it is difficult to simultaneously achieve low thermal conductivity and high compressive strength.

Influence of expandable graphite cladding condition on the performance of carbon-graphite insulation

The internal microscopic morphology of the carbon-graphite insulation material showed the uncoated preform was loose and porous, and most of the holes were irregularly shaped open pores (Figure 8a). After the primary coating of expandable graphite, the number of internal pores of the preform significantly reduced, and open and closed pores existed simultaneously. Moreover, the internal "gullies" of the preform reduced, and the morphology became smoother and flatter (Figure 8b). When expandable graphite was clad two times, the number of holes inside the preform was significantly reduced, the number of pores decreased, and the surface became smoother and flatter. In general, the particle size of expandable graphite considerably influences the degree of expansion and distribution range of pores, and the expandable graphite without cladding and crushing treatment exhibits a large particle size, high degree of expansion, and small expansion range at a high temperature (800°C). Thrust causes the graphite carbon layer to expand outward, resulting in a larger number of non-closable holes in the precast body [15]. In contrast, the expandable graphite subjected to cladding and crushing has a smaller particle size and wider distribution, and the impact force of the expansion process is dispersed. As the phenolic resin adheres to the material surface, its adhesion to the graphite sheet increases; it becomes difficult to expel the gas during the expansion process, and more closed gas holes are produced. Yang et al. used Madagascar purified graphite as the raw material to prepare high-rate expandable graphite and conducted expansion experiments on expandable graphite with different grain sizes to measure the volume after expansion at 850°C. The results showed that, for the same mass of graphite, a larger graphite sheet corresponded to a larger expansion volume of the expandable graphite, and the expansion volume of+0.300 mm grain size expandable graphite was four times larger than that of the expandable graphite with a grain size of minus-0.150 mm, with a value of up to 480 m $L{\cdot}g^{-1}$ [16]. Zhang et al. demonstrated that expanded graphite consists of a number of "microcells" connected to form a macroscopic graphite worm, with irregular elliptical pores in the microcells. The microcellular structure has many tiny pores at the microscopic level, forming a unique and rich pore structure of expanded graphite [17]. This aspect is in accordance with the microstructure shown in Figure 8.

Figure 9a shows the effect of the number of expandable graphite cladding treatments on the porosity, open porosity, and closed porosity of the carbon-graphite insulation. The porosity and closed porosity increased with the number of wraps, whereas the open porosity tended to decrease. The preform porosity, open porosity, and closed porosity were 56.754%, 28.741%, and 27.762%, respectively, when cladding was performed twice. The proportion of the closed porosity was 48.92%, slightly lower than that of the open porosity. After coating treatment, the surface of expandable graphite shows a spheroidizing trend (see Figure 7), which made it easier for the pores between the graphite flakes to be filled. Moreover, because the surface was covered with phenolic resin, the connection state between the expandable graphite and surrounding graphite flakes was modified, which enhanced the bonding ability and created more favorable conditions for the high-temperature expansion to produce closed pores. In addition, the volume shrinkage of the phenolic resin residue at high temperatures (approximately 2%) facilitated the formation of closed pores. The compressive strength of the carbon graphite insulation increased with the number of wraps, whereas the thermal conductivity gradually decreased, with values of 16.432 MPa and 0.743 $W{\cdot}m^{-1}\ K^{-1}$, respectively, after two wraps (Figure 9b). It is worth pointing out that the amount of expandable graphite added is not the better. It was found that, when expandable graphite was added at more than 2%, the carbon-graphite insulation cracked after charring, as shown in Figure 10.

After two cladding treatments of the expandable graphite, the proportion of closed porosity of the carbon-graphite insulation considerably increased. The compressive strength slightly increased, and the thermal conductivity significantly reduced, thereby achieving the synergy of the technical objectives of a low thermal conductivity and high compressive strength.

Thermal and mechanical modeling of carbon-graphite insulation

Various models have been developed to predict the effective thermal conductivity of porous materials, with representative models being the Maxwell-Eucken and EMT equations. The Maxwell–Eucken model [18] assumes the dispersed phase involves spherical particles irregularly dispersed in a continuous phase without contact with one another, and the equations can be expressed as Equations 1 and 2. The EMT equation [19] assumes that, in a composite system, either the components or the filler are surrounded by a homogeneous effective medium. The thermal conductivity of the effective medium is the thermal conductivity of the composite system, and the equation can be expressed as Equation 3.

Maxwell–Eucken 1:

$$k_e = k_1 \frac{2k_1 + k_2 - 2(k_1 - k_2)v_2}{2k_1 + k_2 + (k_1 - k_2)v_2} \quad \textbf{Equation 1}$$

$$k_e = k_2 \frac{2k_2 + k_1 - 2(k_2 - k_1)(1 - v_2)}{2k_2 + k_1 + (k_2 - k_1)(1 - v_2)} \quad \textbf{Equation 2}$$

$$k_e = \frac{1}{4}\left((3v_2 - 1)k_2 + [3(1 - v_2) - 1]k_1 + \sqrt{[(3v_2 - 1)k_2 + (3(1 - v_2) - 1)k_1]^2 + 8k_1k_2}\right) \quad \textbf{Equation 3}$$

where k_e is the effective thermal conductivity of the porous insulation, k_1 is the graphite phase thermal conductivity(5.6 W·m^{-1} K^{-1}), k_2 is the air thermal conductivity (0.026 W·m^{-1} K^{-1}), υ_1 is the graphite phase volume fraction, and υ_2 is the volume fraction of air.

The porous carbon-graphite insulation is considered a two-phase system consisting of a carbon-graphite skeleton and air. Figure 11 shows a comparison of the three thermal conductivity models, and the experimental data were obtained in this study. The experimental data lie in between those of the EMT equation and Maxwell-Eucken 2, and the relative thermal conductivity is lower than the value predicted using the EMT equation. This phenomenon occurs because the effective thermal conductivity depends on the porosity and microstructure of the two phases. In the carbon-graphite insulation, the dense graphite/phenolic resin skeleton is the continuous phase, and air is the dispersed phase. The phenolic resin has a lower thermal conductivity than natural scale graphite and produces a large number of pores during pyrolysis, which reduces the average free travel of phonons during heat transfer. Moreover, the expandable graphite produces a large number of small closed pores, which reduces the point contact within the carbon-graphite insulation and solid phase heat transfer within it.

To clarify the relationship between the compressive strength and porosity, the experimental data were validated using the power function and logarithmic, exponential, and linear models proposed by Balshin, Schiller, Ryshkewitch, and Hasselman [20]. The models are defined in the following equations, and the fitting results of these models to the experimental data are shown in Figure 12.

Ryshkewitch equation:

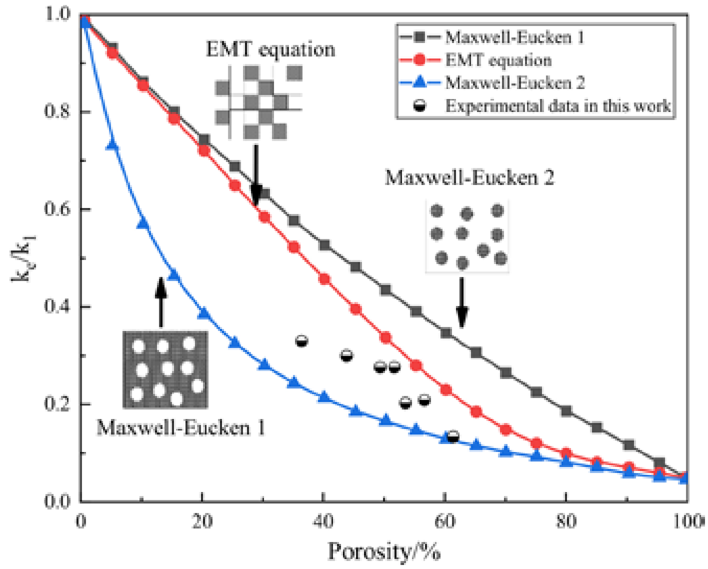

Figure 11: Comparison of the three thermal conductivity models (k_2/k_1 = 20) and the experimental data presented here.

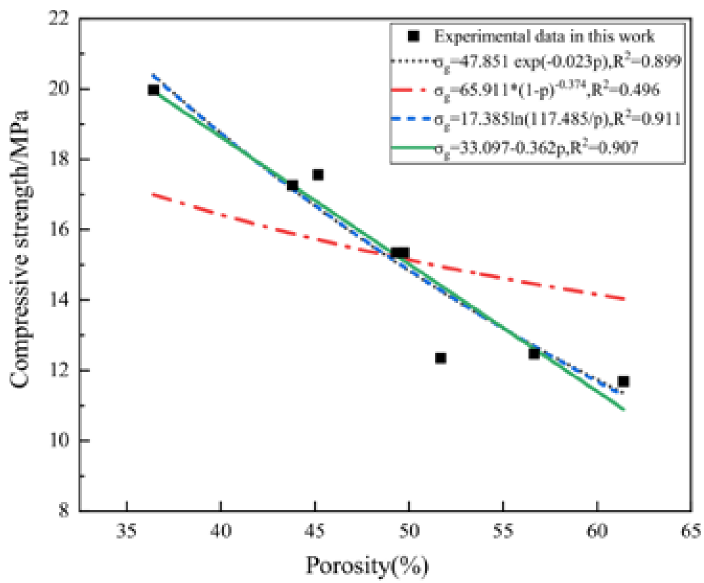

Figure 12: Results of fitting the four mechanical models to the experimental data in this article.

$$\sigma_g = \sigma_0 \exp(-np) \quad \textbf{Equation 4}$$

Balshin's power function model:

$$\sigma_g = \sigma_0 (1 - P)^n \quad \textbf{Equation 5}$$

Schiller's logarithmic function model:

$$\sigma_g = n \ln\left(\frac{\sigma_0}{p}\right) \quad \textbf{Equation 6}$$

Hasselman's linear relationship between the strength and porosity of refractory materials:

$$\sigma_g = \sigma_0 - np \quad \textbf{Equation 7}$$

where σ_g is the compressive strength of the carbon-graphite insulation (MPa), σ_0 is its theoretical strength in the non-porous state, p is the porosity, and n is an empirical constant.

Figure 12 shows that the correlation coefficients of the experimental data with three empirical models are high (0.899, 0.911, and 0.907), although the fitting with the power function model proposed

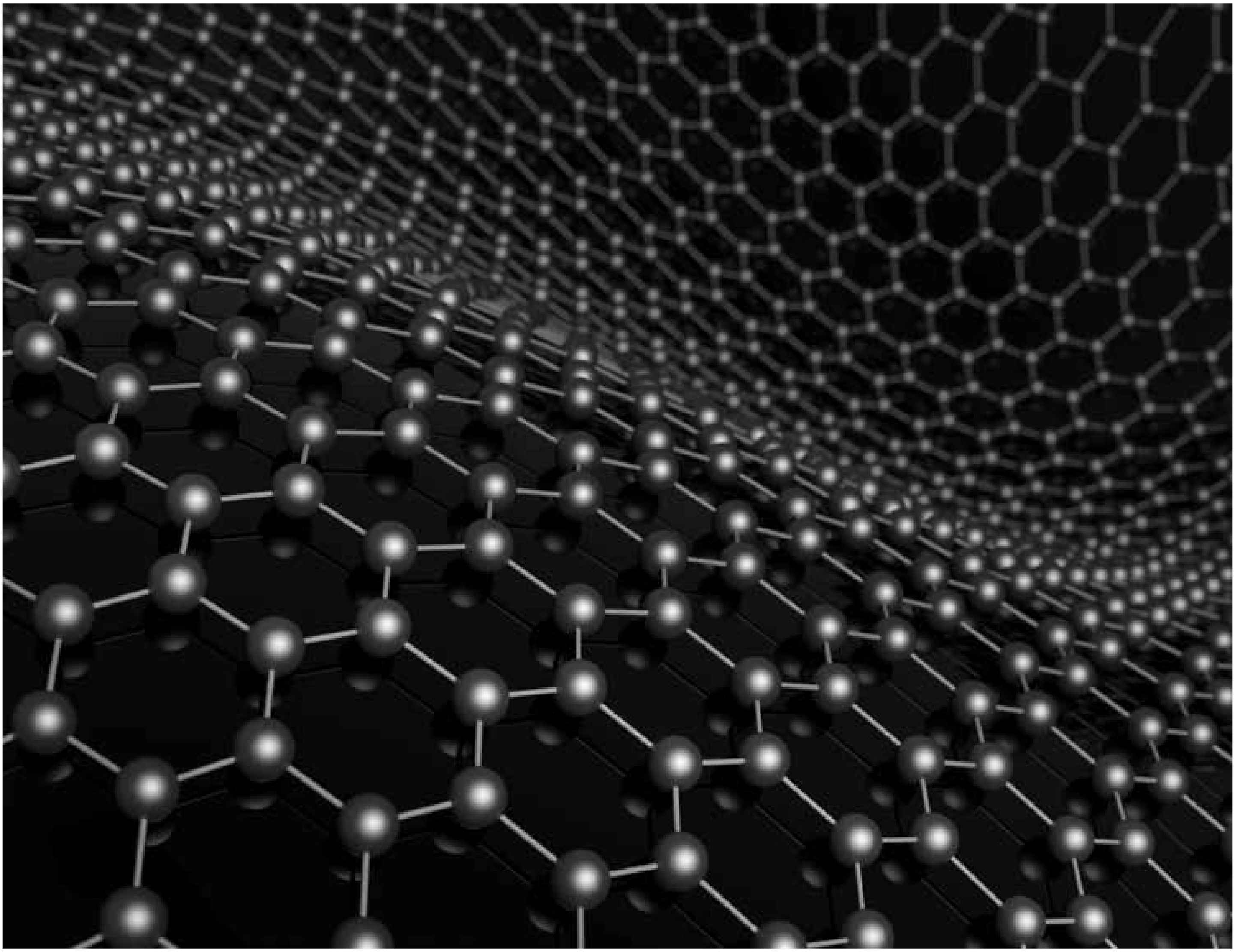

Material composition	Forming methods	Density / (gcm^{-3})	Thermal conductivity / ($Wm^{-1}K^{-1}$)	Compressive strength /MPa	References
Expandable graphite / Alumina fibre Aluminium silicate	Press forming		0.10	0.74	[21]
Hollow balls Al_2O_3-SiO_2	Gel-casting	1.09	0.13	15.0	[22]
Carbon fibre / Graphite fibre	High temperature graphitization treatment	0.16	0.14	2.0	[23]
Graphite felt core / Graphite paper Carbon Fiber	Chemical vapor deposition	0.31	0.40		[7]
This work	Micro-thermal press additive manufacturing	1.20	0.74	16.4	

Table 4: Comparison of overall performance with various lightweight insulation materials.

by Balshin (R^2=0.496) is low. This finding shows the experimental data obtained in this study fit well with all equations except for the power function model. Notably, the porosity and compressive strength are negatively correlated, and the compressive strength progressively decreases with increasing porosity. The data presented in the previous section are consistent with this trend. When the expandable graphite is not pre-treated with cladding, the closed porosity generated within the carbon-graphite material by the cladding treatment is considerably greater (approximately 10%) than that produced when the carbon-graphite material is not clad, accompanied by a small increase in the compressive strength (approximately 7.08%). Future work must be aimed at modeling the effect of closed pores on the mechanical properties of porous insulation materials.

A comparison of the low thermal conductivity and high-strength carbon-graphite insulation prepared in this study and other lightweight insulation materials is shown in Table 4. The carbon-graphite insulation material exhibits a higher compressive strength than other lightweight insulation materials, although its thermal conductivity is slightly higher. Future work can be aimed at reducing the forming density of graphite parts, increasing the porosity of graphite parts, and further reducing the thermal conductivity of the carbon-graphite insulation while maintaining its compressive strength.

CONCLUSION

Carbon-graphite thermal insulation materials with synergistic functional objectives such as a low weight, thermal insulation, high compressive strength, and high-temperature resistance were prepared by micro-thermal pressing additive manufacturing technology. The creation of closed pores in the carbon-graphite insulation material can modify the compressive strength and thermal conductivity of the material, specifically, a reduction in the thermal conductivity and enhancement in the mechanical properties. With the increase in the forming density and addition of thermosetting phenolic resin, the porosity and open porosity of the carbon-graphite insulation materials decreased, whereas the proportion of the closed porosity, compressive strength, and thermal conductivity increased. Increasing the forming density of the carbon-graphite insulation had a more notable effect on the thermal conductivity, whereas increasing the amount of added thermosetting phenolic resin had a more significant effect on the compressive strength.

The creation of closed pores inside the carbon-graphite insulation material can adjust its compressive strength and thermal conductivity in both directions, reducing its thermal conductivity and improving its mechanical properties. By fitting the experimental data, the thermal conductivity model and mechanical model suitable for carbon-graphite thermal insulation materials were obtained.

ACKNOWLEDGEMENTS

This study was supported by the National Natural Science Foundation of China (51575313) and the State Key Laboratory of Material Forming and Mould Technology, Huazhong University of Science and Technology Open Project Research Fund (P2020-003).

DECLARATIONS

Conflict of interest: The authors declared that there is no conflict of interest.

ADDITIONAL INFORMATION

Handling editor: Jaime Grunlan.

PUBLISHER'S NOTE

Springer Nature remains neutral with regard to jurisdictional claims in published maps and institutional affiliations.

REFERENCES

[1] Pulci G, Tirillò J, Marra F, Fossati F, Bartuli C, Valente T (2010) Carbon–phenolic ablative materials for re-entry space vehicles: manufacturing and properties. Compos Part A-Appl S 41:1483–1490

[2] Yang YZ, Yang JL, Fang DN (2008) Research progress on thermal protection materials and structures of hypersonic vehicles. Appl Math Mech 29:51–60

[3] Li TQ, Xu ZH, Hu ZJ, Yang XG (2019) Application of a high thermal conductivity C/C composite in a heat-redistribution thermal protection system. Carbon 48:924–925

[4] Guo (2019) Preparation of new low density C/C thermal insulation material. PhD Dissertation ,Central South University

[5] Lin Y, Liu B, Fei CW (2021) Study on impact resistance of C/SiC ceramic matrix composites for thermal protection of the aerospace vehicle. Math Probl Eng. https://doi.org/10.1155/2021/6255014

[6] Yang XG, Sun YT, Shi DQ, Liu JL (2011) Experimental investigation on mechanical properties of a fiber-reinforced silica aerogel composite. Mat Sci Eng A-Struct 528:4830–4836

[7] Wang Y, Chen ZF, Yu SJ, Saeed MU, Luo RY (2016) Preparation and characterization of new-type high-temperature vacuum insulation composites with graphite felt core material. Mater Design 99:369–377

[8] Wu XW, Luo RY (2011) Mechanical properties investigation of carbon/carbon composites fabricated by a fast densification process. Mater Design 32:2361–2364

[9] Han MK, Yin XW, Chen LF, Rena S, Li ZK (2016) Effect of core-shell microspheres as pore-forming agent on the properties of porous alumina ceramics. Mater Design 113:384–390

[10] Chen S, CaiWH WuJM, Ma YX, Li CH, Shi YS, Yan CZ, Wang YJ et al (2020) Porous mullite ceramics with a fully closed-cell structure fabricated by direct coagulation casting using fly ash hollow spheres/kaolin suspension. Ceram Int 46:17508–17513

[11] Wu HH, Chen K, Li YF, Ren CQ, Sun Y, Huang CH (2020) Fabrication of natural flake graphite/ceramic composite parts with low thermal conductivity and high strength by selective laser sintering. Appl Sci-Basel. https://doi.org/10.3390/app10041314

[12] Guo XB (2018) Preparation and properties of mesophase pitch based carbon / Carbon Composites .PhD Dissertation, Aerospace Power Technology Research Institute

[13] Li SS (2011) Preparation and oxidation resistance of carbon graphite materials. PhD Dissertation, Hunan University

[14] Zhong J, Guo HM, Xie Z, Zhao SM (2018) Firing mechanism of oxide-carbon refractories with phenolic resin binder. Ceram Int 44:5594–5600

[15] Qi MM (2017) Study on microstructure regulation and properties of carbon composites.PhD Dissertation, TianJin University

[16] Yang L, Zhang LY, Qiu YS, Wang J (2019) Preparation and study of expansible graphite from madagascar. Bull Chinese Ceramic Soc 38:3320–3325

[17] Zhang HG(2007) Study on sulfur free and ash free expandable graphite.Master Dissertation, QingDao University

[18] Gong LL, Wang YH, Cheng XD, Zhang RF, Zhang HP (2013) Thermal conductivity of highly porous mullite materials. Int J Heat Mass Tran 67:253–259

[19] Hashin Z, Shtrikman S (1962) A variational approach to the theory of the effective magnetic permeability of multiphase materials. J Appl Phys 33:3125–3131

[20] Odler I (1991) Strength of cement (final report). Mater Struct 24:143–157

[21] Fang K (2016) Study on preparation and performance of an alumina-fiber-based expandable insulation material. Master Dissertation, China Building Materials Research Institute

[22] Huang CS (2011) Preparation and property study of porous lightweight mullite ceramics. TianJin University, Master Dissertatio

[23] Friedrich W, Qian CS, Wang YH (1983) High temperature insulation material made of carbon fiber and graphite fiber. Carbon Tech 03:11–13

ABOUT THE AUTHORS

Junchao He, Haihua Wu, Lei Zhong, Qiang Zhong, Xicong Ye, Zhi Liu, and Yi Kang are with the Graphite Additive Manufacturing Technology and Equipment Engineering Research Center, China Three Gorges University, Yichang, China. Qiang Yang is with the State Key Laboratory of Mechanical Manufacturing System Engineering, Xi'an Jiaotong University, Xian, China.

The article has been edited to conform to the style of *Thermal Processing* magazine.

HEAT TREAT EVENTS 2023

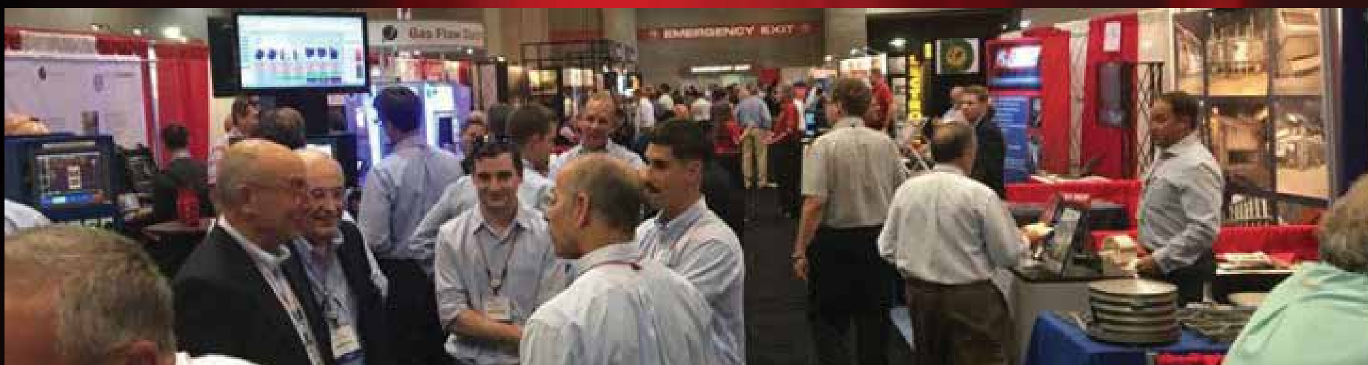

AEROMAT 2023 › March 14–16 | Fort Worth, TX

Heat Treat Mexico 2023 › March 28–30 | Monterrey, Mexico

Ceramics Expo 2023 › May 1–3 | Novi, MI

Rapid + TCT 2023 › May 2–4 | Chicago, IL

AISTech 2023 › May 8–11 | Detroit, MI

Forge Fair 2023 › May 23–25 | Cleveland, OH

PowderMet 2023 / AMPM 2023 › June 18–21 | Las Vegas, NV

IFHTSE World Congress › Sept 30–October 3 | Cleveland, OH

FABTECH 2023 › September 11–14 | Chicago, IL

IMAT 2023 › October 16–19 | Detroit, MI

Heat Treat 2023 › October 17–19 | Detroit, MI

Global Materials Summit › December 5–7 | Naples, Florida

Thermal processing

Look for bonus distribution of *Thermal Processing* at many of these shows. And we look forward to seeing you at select events this year.

HOW TO TAME A PLASMA

POWER-DELIVERY SOLUTIONS FOR TOP PROCESS ISSUES

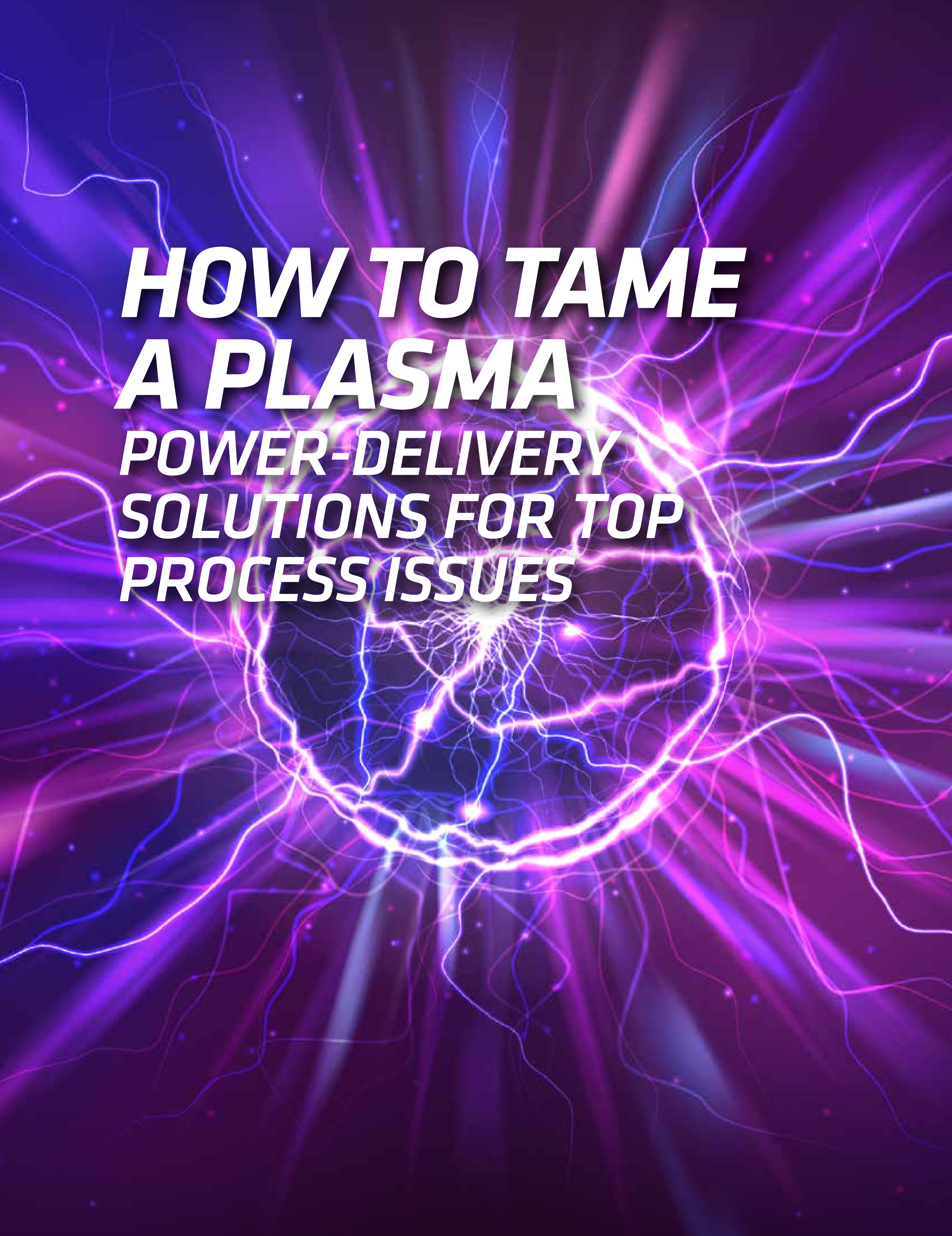

The ability to establish and maintain a stable plasma hinges on choosing the right power supply for your application and process.

By DHAVAL DHAYATKAR

Film quality, throughput, yield, etch uniformity, and sidewall control all depend on the ability to ignite, maintain, and control a stable plasma. Precise, nimble power delivery is crucial. Extremely tight accuracy is required for the stringent multi-step manufacturing processes that deposit or etch material to produce near-flawless nanostructured films on a fragile glass substrate or transform a silicon wafer into thousands of microcircuits and billions of transistors — potentially worth hundreds of thousands of dollars.

The application-specific requirements of etch and deposition processes demand a wide range of products and capabilities that can operate with exceptional reliability and stability, addressing specific challenges of fabricating nano- and micro-scale electronics. Plasma characteristics are dynamic; power supplies must continuously respond to instant changes to support a stable plasma, while fulfilling the performance requirements of the specific process recipe. These recipes could include hundreds of steps, each requiring different plasma conditions in quick succession; as such, the capability to shape plasma characteristics quickly and precisely becomes more and more critical. The power supply's inherent topology, algorithms, controls, and sensor capabilities determine its ability to perform within these extremely tight parameters.

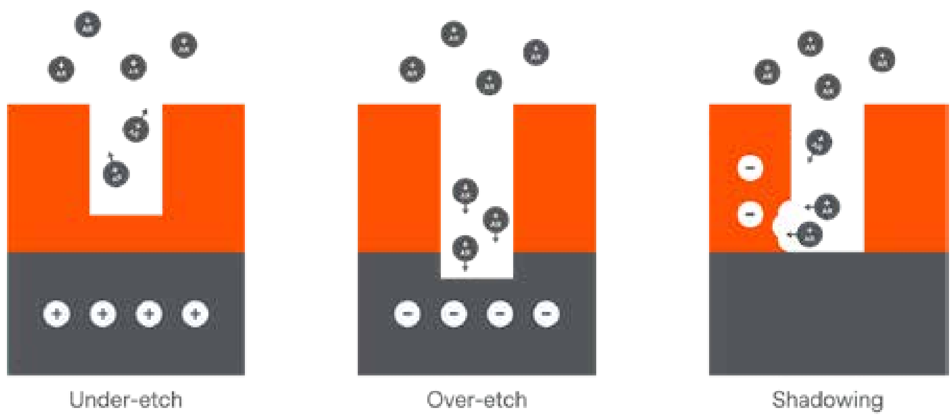

Figure 1: Paschen curve.

PLASMA IGNITION AND MAINTENANCE

The initial voltage required to ignite a plasma depends on many factors, including chamber geometry, gas chemistry, pressure, temperature, and other conditions. For example, the Paschen curve shown in Figure 1 illustrates the dependence of ignition voltage on pressure and distance between electrodes for DC breakdown.

To reliably and repeatably achieve plasma ignition, the power supply should be able to deliver a precise voltage "spike" within these parameters. This accelerates the electrons within the plasma chamber, providing enough kinetic energy to collide with and ionize the process gas atoms or molecules. An initial number of free electrons collide with additional atoms to release further electrons, creating an avalanche effect.

Once the correct conditions are achieved, ignition occurs in a matter of microseconds to milliseconds, causing drastic changes in the process environment, including impedance. Because the voltage required to sustain a plasma is less than that required to ignite it, the power supply must react almost instantaneously to decrease voltage to processing levels. Without a high degree of speed and responsiveness, the plasma can extinguish or become unstable. Plasma impedance is highly dynamic, and significant changes can occur. For example, it may change during ignition when pressure variations (gas dissociation) occur as the system stabilizes, when system drift occurs as electrodes are heated over time, and under other conditions.

Today's advanced power supplies are able to swiftly and continuously react to conditions within the process environment to support plasma stability. The graphic in Figure 2 illustrates the closed-loop relationship in an RF-powered process between plasma characteristics and power-delivery precision and responsiveness, which applies both to the pre- and post-ignition phases; dP represents incremental changes in delivered power that affect plasma properties, such as impedance, dZ. In turn, changes to the plasma environment necessitate changes to power delivery.

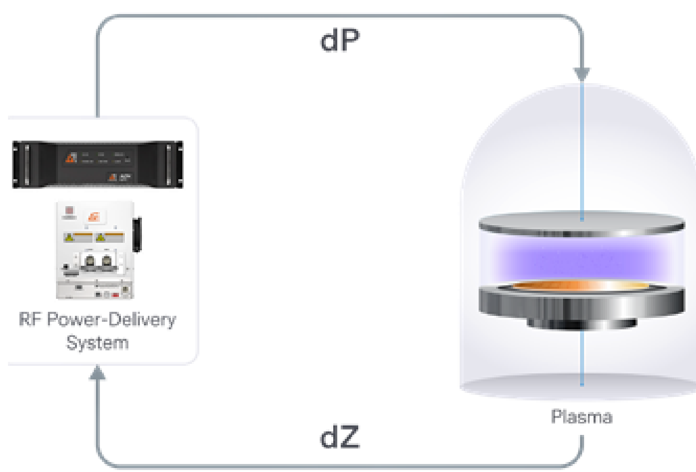

Figure 2: Simplified illustration of the closed-loop relationship between power delivery and plasma characteristics.

The plasma-power generator must both optimize power delivery considering known factors and respond almost instantaneously to a dramatic shift in conditions within the chamber once the plasma ignites. For example, empirically determined match-network presets "predict" the impedance of the plasma before it ignites.

Speed and agility are key not only to immediately post-ignition, but also throughout processing — with different requirements depending on the process type and during any type of transition within an active plasma process.

PLASMA-ENHANCED CHEMICAL VAPOR DEPOSITION (PECVD)

In multi-step PECVD processes for semiconductor manufacturing where every nanometer matters, the RF power supply must react in microsecond time scales to changing process environments as described above. In a PECVD process, chemical reactions inherent in this deposition technique cause plasma impedance fluctuations as new process gases are introduced and residual contaminants are pumped out. As chip architectures become smaller and more complex, the production process steps become shorter and more frequent and the power supply, too, must be more agile to maintain the specific plasma characteristics required for a given process step and application.

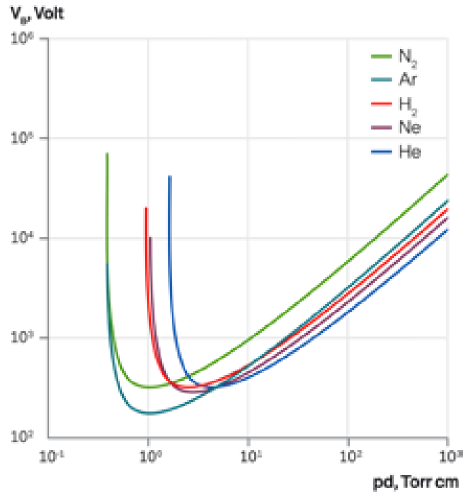

Figure 3: Simplified illustration of the relationship between charge buildup and etch issues.

ETCH

As device structures shrink, etch dimension precision, profile/uniformity control, and end-point detection become increasingly critical. Similar to PECVD processes, the ability of an RF power system's impedance matching algorithms to quickly and continuously tune power delivery to match the dynamically changing complex impedance of the plasma is key in etch processes. Besides plasma changes, etch surfaces also undergo dynamic electrical and chemical changes as they are depleted of material, which can affect power-delivery stability. As in any RF-powered process, but especially with the unique factors within etch applications, fast tuning algorithms are key to responding quickly and precisely adapting power delivery to maintain process stability and ensure maximum power delivery into the process environment.

Etching of contact holes or high-aspect-ratio trenches, especially on insulating materials, can be accompanied by undesired charging effects that are responsible for micro-trenching, notching or twisting of structures, which in turn negatively affect component performance. Charge accumulation generates electric fields that can distort incoming ion trajectories and can lead to breakdown of the dielectric layer. Power-modulated/pulsed plasma with a variety of pulsing combinations (source, bias, synchronous etc.) has been used to control radical/ion fluxes and energies to optimize conditions to resolve above challenges. (Figure 3)

Pulsing also allows access to energy regimes that typically are not available with continuous wavelength (CW) operation, providing more precise control of certain etch and species (byproducts) and thus better uniformity. It enables control of the ratio of high- and low-energy ions, as well as manipulation of ion-energy distribution function (IEDF) outside of allowed limits for CW.

PHYSICAL VAPOR DEPOSITION (PVD)

Demanding applications, such as the following, require the power supply react to process instabilities in microsecond time scales:

» Deposition of high-quality TCO coatings, such as ITO, IGZO, AZO, etc., from multicomponent targets on flexible/heat sensitive substrates.

» High-hardness coatings, such as metal nitrides and carbides on work pieces.

» Large-area coatings of uniform and defect-free insulating materials such as SiO2 and TiO2.

» Decorative coatings with high-quality color and surface finish.

To maintain plasma stability and deposition quality, the power supply must be able to regulate multiple parameters, including power, voltage, and current, while adjusting power delivery within a fraction of a millisecond.

ARC MANAGEMENT

Arcing is a common form of plasma instability in deposition processes that happens when built-up charges around oxides or inclusions on a target surface suddenly discharge. If not managed quickly and effectively, this can have potentially devastating effects, including substrate (cracks, defects at edges), target (nodules formation), and equipment damage. When an electrical discharge occurs, the arc can eject particulates from the target, which can cause film damage such as macroparticles, pinholes, inclusions, and other structural surface defects. Arcs also can drain energy from the total amount supplied to plasma system.

Several aspects of a process affect arc rates and arc energy, including delivered power level, target material, process gas, chamber geometry, and other factors. Though various aspects of the plasma system can lead to arcing, the power supply is key to minimizing process disturbances associated with damage, with different functionality depending on process-power type.

ARC DETECTION AND HANDLING

Monitoring of both current and voltage enables today's plasma power generators to detect an arc quickly and accurately. A robust modifiable arc management procedure should be available to users so that they can manage the arc treatment according to their specific requirements. Especially in reactive sputtering of dielectric material, pulsing and proper arc management have led to strong reduction in arc-related damage on coatings.

In a DC-powered process, during an arc event, changes in plasma impedance cause the output voltage to quickly approach zero, while the output current significantly increases. An increase in voltage and/or current beyond a defined limit or set of threshold criteria initiates an immediate power-supply response. In as little as 1 µsec, the power supply first reverses voltage to swiftly dissipate the current driving the arc, dropping to zero A in a 3-to-4 µsec timeframe.

This voltage reversal is followed by a shutdown phase during which power delivery ceases. The duration of the shutdown is brief (tens of micro-seconds) and precisely timed to completely extinguish the arc without causing process instabilities that could affect throughput and yield. If this response is successful, the event is called a micro-arc. However, if the arc persists, it is termed a hard arc, and the power supply shuts off for a progressively longer duration until the plasma stabilizes. The ability to adapt to specific process conditions helps minimize power-delivery shutoff time to maintain delivered power and throughput. In addition, power supplies that are able to slowly ramp energy back up after an arc-response shutdown reduce the likelihood that the arc will be re-ignited by applying too much energy too soon.

RF processes are typically less susceptible to arcing than DC due to the nature of the technology; however, certain arc management algorithms exist for particularly arc-prone processes.

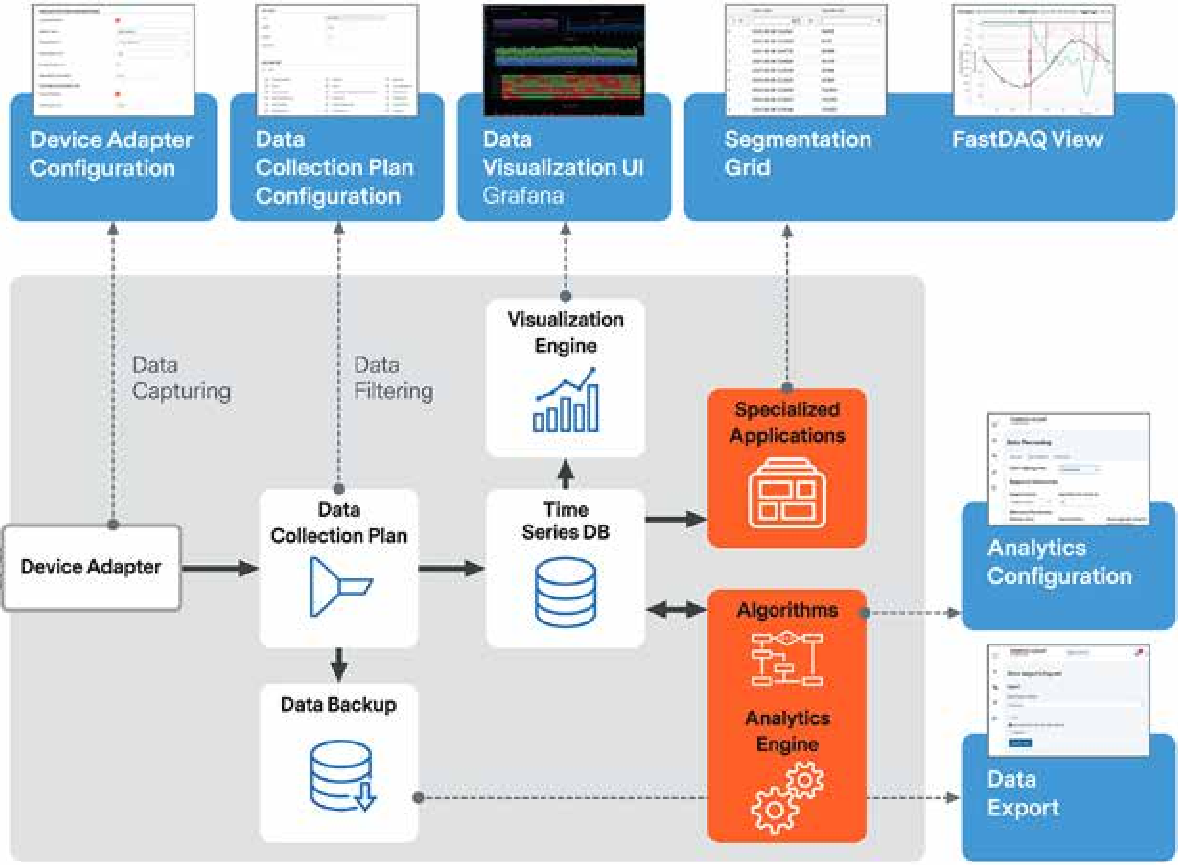

Figure 4: PowerInsight by Advanced Energy™ data acquisition and analysis platform functional architecture.

ARC ENERGY

Current market demands for higher throughput are raising the pressure to increase process power levels. However, as process power levels increase, arc energy (expressed as mJ per kW) also increases because the energy available to an arc is determined by the energy stored in the output of the power supply plus that stored in the cabling. Providing less power to the arc reduces the likelihood it will cause damage before the power supply's response can extinguish it. Therefore, power supplies designed to minimize stored energy generally are associated with less arc damage within the process.

ARC PREVENTION

Bipolar DC technology, typically used in PVD processes for industrial coatings, can neutralize and/or prevent charge buildup by dissipating it on the reverse pulse. This regularly shuts plasma off by reversing voltage (for example, every 50 kHz) to clear "hot spots" on the target. While pulsing benefits processes by using time dependencies to enhance effects (e.g., broad energy distribution of electrons at the start of the pulse), the periodic reversal of voltage of an electrode helps clear charge buildup and thereby arcing.

Though RF-powered processes typically are less prone to arcing, pulsing also can prevent charge buildups that lead to damaging electrical discharges in these applications.

PROCESS VISIBILITY

Access to high-resolution data and analysis opens a window into actual conditions within the plasma system in real time, providing insight into power-supply and process performance. DC and RF power supplies that come with embedded or optional add-on solutions for data acquisition, as well as available data analysis consultation, enable process operators maintain a more stable, repeatable plasma and process. Browser-based dashboards, high-data resolution, and sophisticated algorithms increase the speed and accuracy of process fingerprinting and root-cause analysis of process deviations, helping users pinpoint ways to resolve existing issues and visualize previously unidentified optimization opportunities.

Such a platform can expand process, machine, and quality data along five key parameters:

- Visibility.
- Resolution.
- Accuracy.
- Aggregation.
- Analysis.

With the unique knowledge provided by this solution, plasma process operators can pinpoint ways to stabilize the plasma and process and visualize previously unidentified optimization opportunities over the long term. (Figure 4)

CONCLUSION

The ability to establish and maintain a stable plasma hinges on choosing the right power supply for your application and process — not only the right type of power, but a unit that can provide features and functionality for specific film quality, etch quality, throughput, and yield requirements. Power-delivery agility and plasma control are increasingly critical, especially in semiconductor applications as device architectures shrink, processes transitions become faster, and recipes become more complex. With high-quality topologies, fast algorithms, sophisticated controls, and extensive sensor capabilities, the most advanced power supplies keep pace with today's quickly evolving technologies.

ABOUT THE AUTHOR

Dhaval Dhayatkar is senior director of marketing at Plasma Power.

INDUSTRIAL PHYSICS

GLOBAL TEST AND INSPECTION PARTNER

For the heat-treating industry, Industrial Physics provides key solutions for thermal logging and gas analysis. (Courtesy: Industrial Physics)

By providing test and inspection solutions across a wide range of specialized applications, Industrial Physics is able to protect the integrity of packaging, products, and materials for manufacturers, production lines, and laboratories all over the world.

By KENNETH CARTER, Thermal Processing editor

The proper testing and inspection of products can make or break a company, so it's essential those important tasks are done correctly and efficiently.

With a century's worth of experience, the minds behind Industrial Physics and its group of specialist testing brands, including TQC Sheen, C&W Equipment, Systech Illinois, Eagle Vision, and many more, have been ensuring the integrity of brands and products for customers across a huge gamut of industries, including heat treating.

"That means working with manufacturers, production lines, and laboratories with their R&D and quality control needs across a wealth of different industries all over the world," said Nico Frankhuizen, manager of product management at Industrial Physics. "With the power of Industrial Physics, the scope is enormous. We could be dealing with companies that operate within the food and beverage industry, to metal packaging, to flexible packaging, to inks and coatings, to pharmaceuticals, to medical devices, to electronics, and to many more."

BRAND REPUTATION

This assurance that materials are being protected is essential to keeping brand reputation intact, according to Frankhuizen.

"Obviously big brands really don't want to damage their reputation or lose out on money, and it's our job to prevent any risks within this area; we do this by providing a range of different products that support a variety of testing needs," he said. "One of our specialist testing brands, TQC Sheen, offers highly extensive scope equipment for the inks and coating space. From abrasion testing, to gloss testing, to appearance analysis, we have a wealth of solutions on offer."

Specifically for the heat-treating industry, Industrial Physics provides key solutions for thermal logging and gas analysis, according to Frankhuizen. In particular, Industrial Physics' TQC Sheen CurveX 4 and CurveX Nano Oven Logger kit have energy-saving properties.

"Our TQC Sheen CurveX range offers manufacturers that use industrial ovens a highly effective method of reducing energy consumption, optimizing production processes, and delivering a rapid return on investment," he said. "The information generated by the data loggers allows users to fully understand how efficiently their oven and production processes are running."

The equipment calculates the provided energy levels to the heat-treatment process in order to make sure the customer isn't wasting money and the process is handled efficiently, according to Frankhuizen.

OXYGEN GAS ANALYZERS

Systech Illinois — another specialist testing brand belonging to the Industrial Physics group — offers process oxygen gas analyzers that allow customers to save on their inert-gas consumption by maintaining the correct climatic conditions within their ovens, according to Frankhuizen.

"Ultimately, these advanced solutions allow customers to make more accurate decisions that save resource, energy, and ultimately money." he said.

Industrial Physics' TQC Sheen CurveX4 and CurveX Nano Oven Logger kit has energy-saving properties. (Courtesy: Industrial Physics)

INTEGRITY PROTECTION

And all that technological expertise circles back to Industrial Physics' core purpose, which is to protect the integrity of its customers' brands and products.

"We do that across all of our different testing solutions," Frankhuizen

Several probes for measuring the ambient temperature and the temperature of the product can be connected to the CurveX4 data logger. (Courtesy: Industrial Physics)

said. "And that would be no different within the heat-treatment industry. We're there to protect and to make sure that quality is upheld. Really, it's all about the protection for our customers."

And as the world has advanced, Frankhuizen emphasized that Industrial Physics has kept pace along with it.

"I think as the world evolves, technology evolves and instruments advance," he said. "Across the entire landscape of Industrial Physics, our instruments have advanced. We have got some of the best experts in the world at Industrial Physics within the world of testing. And we have so many different products that I think we're able to make sure that we're offering products with the best quality. Our products have more advanced solutions that mirror the industry's overall evolution. It allows for more precise analysis, and that also allows for a safer and more stable production environment for our customers."

WORKING WITH CUSTOMERS

To maintain that integrity with its customers, Frankhuizen said it's important that the company work closely with their customers to directly address any challenges that may arise.

"We would look at the issue and the analysis that's required," he said. "We have a plethora of different products on offer, but it's really about making sure that we're fully understanding every single customer's need and getting to grips with exactly what it is that they're trying to achieve. We're passionate about making sure that we're not just a provider of products, but a true partner — all of our team are actively working with our customers to look at all of the different testing techniques and testing solutions that we have in order to find the right one for them."

That collaboration with a customer is critical, according to Frankhuizen.

"We don't purely look at the specifications of the process, but the culture in the company — what it is that they need on many different levels — then we help find a solution for them." he said.

Those types of customer services have helped Industrial Physics maintain its success during its path to become a large collaborative organization, according to Frankhuizen.

"By bringing all of these specialist testing brands together under the Industrial Physics umbrella, we have the combined power of expertise across many different specialisms that support a broad range of industries — this allows us to offer a truly unique approach," he said. "Industrial Physics encompasses all of the power of a global organization, but we have specialists on the ground, and this allows us to be able to offer a truly localized approach when it comes to service."

"A customer could enquire about something really specific within heat treatment, but they might have five other problems that they need to solve in regards to their test and inspection requirements," Frankhuizen said. "We have a wide basket of solutions across a multitude of testing applications that allow us to support customers across a range of industries."

LOOKING TO AN ECO-CONSCIOUS FUTURE

And that will become even more important as the world becomes more energy conscious and eco-friendly, according to Frankhuizen, which means companies like Industrial Physics will need to offer newer and better production principles to go along with those changing standards.

With its CurveX4 and CurveX Nano products, Frankhuizen said Industrial Physics is already on the cutting edge of offering solutions that can cut energy use by implementing an effective method of mitigating the effects of recent energy-price increases.

"Our CurveX solution offers intelligent temperature data logging systems that are specifically designed to provide users with complete profiles about their ovens and advanced insights of their coating productions," he said. "In fact, one of our customers used our solution to reduce their energy consumption by two-thirds."

Reducing fuel usage has helped Industrial Physics' customers meet their environmental commitments by reducing greenhouse gas emission at a time when the United Nations Framework Convention on Climate Change is calling on all nations to address climate change, according to Frankhuizen.

"Industrial Physics' CurveX4 and Curve X Nano Temperate Data Loggers achieve impressive energy-use reductions in industrial ovens by providing highly accurate information about the drying/curing time of the products," he said.

MORE INFO industrialphysics.com

MARKETPLACE ///

Manufacturing excellence through quality, integration, materials, maintenance, education, and speed.

Contact **Thermal Processing** at 800-366-2185 to feature your business in the Marketplace.

ADVERTISER INDEX ///

BRIAN KELLY /// APPLICATIONS ENGINEERING MANAGER
/// HONEYWELL THERMAL SOLUTIONS

"We're looking at how our burners can utilize alternate fuels like hydrogen and other alternate fuels that don't have any or as much carbon as natural gas or oil."

What do you do at Honeywell?

I'm part of Honeywell Thermal Solutions. We're a group of companies that Honeywell has acquired over the last couple of decades that included some larger companies in the industrial combustion arena such as Maxon Corporation of Muncie, Indiana; Eclipse Combustion that was based in Rockford, Illinois; Kromschroder out of Lotte, Germany; and Hauck Manufacturing that was out of Pennsylvania. As Honeywell Thermal Solutions, we supply safe, efficient, and sustainable thermal solutions for industrial applications. Just about any industrial process that needs heat, that's where we fit.

My role at Honeywell Thermal Solutions is applications engineering manager. I tell people that my job is to keep the company out of trouble. My group advises our sales engineers, engineering group, as well as our customers on the application, design, and control of thermal systems to achieve the required goals. We supply a hundred different type burners for a lot of different applications from high to low temperature.

There's been an industry-wide drive to lower carbon emissions. What is Honeywell doing to contribute to that goal?

We are doing a lot, actually, and this is in many different divisions of Honeywell as well. From a Honeywell Thermal Solution side of it, we're looking at how our burners can utilize alternate fuels like hydrogen and other alternate fuels that don't have any or as much carbon as say natural gas or oil to reduce CO_2 from the combustion process. We offer products, burners, and systems to fire more efficiently, so they reduce the amount of fuel use that's not only reducing the customer's fuel bill, but it's reducing the carbon going out the stacks.

From an overall organization, there are divisions of Honeywell involved in the development of catalyst systems to drive down the cost to produce green hydrogen as well as carbon-capture technologies and even low carbon sustainable aviation fuels. Honeywell has a commitment to be carbon neutral by 2035, as have many large companies.

How can you reduce pollutants without sacrificing quality and performance?

There is a variety of ways to reduce emissions in thermal processes from burner design, burner control, fuel choice, and overall system design. Depending on the temperature of the process, there are different burner techniques and technologies to reduce emissions like NOx that not only reduce emissions but maintain or even enhance performance. NOx reduction has been one of the biggest focuses of a lot of industry for a long time, and it's getting stricter all over the world. Some of the techniques that are used there are high temp such as staging technologies as well as flameless, where with lower temperature, we can use premix and excess air to reduce those emissions.

Certainly, carbon reduction or neutrality is the focus of almost every industry today. The reduction of CO_2 is only done by reducing the consumption of carbon-based fuels or carbon capture and sequestration. Whatever we can do to reduce that ensures we're running the system more efficiently. We're using less fuel. That happens with self-recuperative burners or using waste heat to preheat the combustion air via heat exchangers to the combustion system. You don't take as much energy to raise the product's combustion up from cold air to the process temperature. That's less energy required, so less fuel used, less emissions coming out on both NOx on a pounds per hour as well as your CO_2. You can also fire the burners in different control methods that can be more efficient, even if you're using a different fuel.

What innovations has Honeywell developed to help deal with this challenge?

It's looking at total emissions, where Honeywell has developed innovations to help with the emissions with more advanced self-recuperative type burners and controls. These are smaller, multiple burners on, say, heat-treat furnaces that preheat the combustion air in a nice package so you don't have to deal with hot air piping and maintenance.

Different designs are getting us lower NOx, but also during the development, they are tested with alternate fuels — fuels that are byproducts of different processes — as well as hydrogen, which has, of course, gotten a lot of talk because it is carbon free. But hydrogen is going to just take you just so far depending on availability, which will continue to increase and cause the price to decrease. Other innovations are control technology as well as connectivity. We've got devices that can be connected and remotely tuned, but also can remotely monitor the health of a customer's burner system or their furnace and can alert them to possible issues. What we see in the industry is less and less combustion expertise/experience at the customer/end-user level, so we see it as an opportunity to assist those customers in maximizing their uptime and therefore profits.

How has Honeywell been able to help your customers obtain this reduction in pollutants such as NOx?

Really it is working with them to learn their processes and applications. Honeywell Thermal has hundreds of years of combustion knowledge and expertise, and this is an advantage to our customers. We can take a consultative approach to their processes. It's our job to work with these customers, to know their applications. This is an exciting time in the thermal processing industry and we will continue to develop and innovate to lead the market and deliver to our customers.

MORE INFO process.honeywell.com


YOU'VE GOT THE PRODUCTS.
YOU'VE GOT THE SERVICES.
NOW, LET US SHARE YOUR STORY.
Thermal Processing wants to make sure the best possible audience knows your company. Through our print, online, and social media presence, our experienced staff can get your message to an industry that wants to know what you can do.
Thermal processing
To learn more, contact national sales director Dave Gomez at dave@thermalprocessing.com or call 800.366.2185 ext. 207

MENTOR®
VACUUM HEAT TREATING FURNACE

HORIZONTAL CAR BOTTOM

VERTICAL BOTTOM LOADING

MENTOR® & MENTOR® PRO

INTERNAL QUENCH

EXTERNAL QUENCH

MENTOR®

The Mentor®, model HFL-2018-2IQ, is a horizontal, front loading, compact, vacuum heat treating and brazing furnace generally designed and developed to accommodate small to mid-size furnace loads in an efficient and economic manner. It is a high temperature, high vacuum, batch-type furnace with electrical resistance heating elements. The Mentor® is mounted on a single, portable platform for easy shipment and maneuverability. Designed for heat treating, hardening, brazing, stress relieving, normalizing, annealing, tempering, sintering, homogenizing, degassing, diffusion bonding, and creep forming.

SOLAR MANUFACTURING

267.384.5040
sales@solarmfg.com

solarmfg.com

Give us a call to learn more about our vacuum furnace ingenuity.

THE BRIGHTEST SOLUTIONS THROUGH INGENUITY

PROUDLY MADE IN THE USA